. . . . . contributing to man's
understanding of the environment World

TECHNICAL REPORT NO. 80-6

AN ASSESSMENT OF THE USE OF STRAIN AND INERTIAL SEISMOGRAPHS TO ENHANCE SEISMIC SIGNAL TO NOISE RATIOS

TELEDYNE GEOTECH

(9) Final rept.)

(12) 86

(18) AFOSR

(19) TR-80-0633

(14) TR-

TECHNICAL REPORT NO. 80-6

(6)

AN ASSESSMENT OF THE USE OF STRAIN AND INERTIAL SEISMOGRAPHS TO ENHANCE SEISMIC SIGNAL TO NOISE RATIOS

(10) G. G. Sorrells
~~and~~
O. D. Starkey

(11) 7 Mar 80

Sponsored by

Advanced Research Projects Agency (DOD)
ARPA Order No. 3291-21 (15)
Monitored by AFOSR/NP under Contract F49620-79-C-0015

ARPA Order-3291

TELEDYNE GEOTECH
3401 Shiloh Road
Garland, Texas 75041

7 March 1980

CONTENTS

ILLUSTRATIONS

ILLUSTRATIONS, Continued

****

TABLES

AN ASSESSMENT OF THE USE OF STRAIN AND INERTIAL SEISMOGRAPHS TO ENHANCE SEISMIC SIGNAL TO NOISE RATIOS

1. FOREWORD

In order to verify compliance with the terms of the proposed comprehensive nuclear test ban treaty, seismic monitoring sites may be located at regional distances from potential test sites. It can be reasonably assumed that some type of signal-to-noise ratio (SNR) enhancement technique will have to be applied to the raw data collected at these sites in order to detect and identify the source of the relatively weak seismic signals generated by low magnitude earthquakes and underground nuclear explosions. In the past, seismic arrays coupled with simple beamforming data processing methods have been used extensively to enhance short period teleseismic SNRs. Utilization of this technique is based upon the observation that in the frequency bandwidth commonly occupied by teleseismic signals, the signal field generally appears to be much better organized than the ambient earth noise. However, recent studies by Mrazek et al (1979) indicate that the lateral decorrelation of regional signal fields is comparable to that of the earth noise field in commonly shared bandwidths. Under these conditions, the use of horizontally distributed arrays, coupled with simple beamforming techniques is not likely to yield significant improvements in regional SNRs. Thus, there is a need to reassess the use of existing SNR enhancement methods as they pertain to the detection and identification of weak regional seismic signals. In this regard it is worthwhile to reconsider the use of linear combinations of the outputs of strain and inertial seismographs to increase regional SNRs. Like seismic arrays this particular method utilizes differences in apparent horizontal wavenumber to separate signals from noise. However, in contrast to arrays, it is insensitive to the effects of lateral signal decorrelation because all necessary observations are made at essentially the same point. Colocation of the sensors may also substantially reduce the potential political, logistical and security problems associated with the operation of a nuclear test monitoring station in a foreign country. Thus, the strain-inertial (S-I) SNR enhancement method seems particularly well suited for use at the treaty verification sites that may be located within the Soviet Union. Unfortunately, previous attempts to utilize S-I methods in the past have met with only limited success and investigations in this area were terminated in the early 1970s (cf. Shopland 1966, 1968, Shopland and Kirklin 1969, 1970). This relatively poor performance has been attributed primarily to the existence of high system noise levels at the output of the strain transducer. However, in retrospect, the failure to recognize and adequately account for the effects of local environmental factors may have played an equally important role in limiting the SNR enhancement capabilities of previously developed S-I systems. Recent progress in the development of high resolution seismic sensors suggests that it may now be possible to substantially reduce the strain system noise problems that plagued earlier attempts to reduce the S-I method to practice. Furthermore, the greater appreciation of the local environmental noise problem that has developed during the past decade leads to the belief that practical methods for minimizing their impact on S-I SNR enhancement capabilities can be developed.

For these reasons AFOSR under the sponsorship of DARPA has authorized Teledyne Geotech to assess the merit of developing an advanced S-I seismograph system to enhance seismic SNRs. The principal results of this assessment are described in the following pages.

2. POTENTIAL P WAVE SNR ENHANCEMENT

2.1 BASIC CONCEPTS

Interest in the strain-inertial SNR enhancement method was triggered by Romney (1964) who presented theoretical arguments to demonstrate that simple subtraction of an appropriately filtered and normalized strain seismogram from a simultaneously recorded inertial seismogram would result in substantial improvements in P wave SNRs, provided that the earth noise consisted principally of single mode Rayleigh waves. The essential elements of his arguments are illustrated by the two sets of curves shown in figures 1-a and 1-b. For the purposes of this illustration we have assumed that vertical strain and displacement observations are made at the surface of a homogeneous, isotropic perfectly elastic half space. We have further assumed that the earth noise consists of Rayleigh waves and that we are interested in enhancing the SNR for a P wave arriving at the observation point with a 20° angle of incidence. The two curves shown in figure 1-a illustrate the relative differences between the strain-displacement response ratios for the Rayleigh wave noise and the P wave signals. These ratios measure the magnitude of the vertical strain per unit of vertical displacement and thus reflect the relative strain sensitivity of the earth to different types of seismic waves. For the purposes of illustration they have been normalized so that the Rayleigh wave strain-displacement response ratio is 1 at a frequency of 1 Hz. Observe that the relative vertical strains for the Rayleigh wave are almost a factor of 10 larger than those for the P wave. This means, in effect, that the output of a vertical strain sensor will be relatively rich in Rayleigh wave noise when compared to the output of the vertical displacement sensor. In other words, the strain output is for all practical purposes, an estimator of the noise observed at the output of the vertical displacement sensor. We may take advantage of this property by filtering the strain output so that it is identical to the displacement output when only noise is present. When this is done the strain displacement response ratios will take the form shown in figure 1-b. From this illustration it can be seen that if the filtered strain output is subtracted from the displacement output the remainder will contain only the signal plus a relatively weak signal distortion term. Such a process is commonly referred to as prediction error filtering and under appropriate background noise conditions this technique can be a powerful tool for seismic SNR enhancement.

In the following sections we shall quantitatively assess the potential SNR enhancement capabilities of a linear combination of the outputs of a vertical strain sensor and a vertical displacement sensor under certain idealized noise conditions. The results of this assessment will not only provide insight into the problems encountered in previous attempts to reduce the S-I method to practice but will also provide basic constraints on the design and utilization of an advanced S-I system.

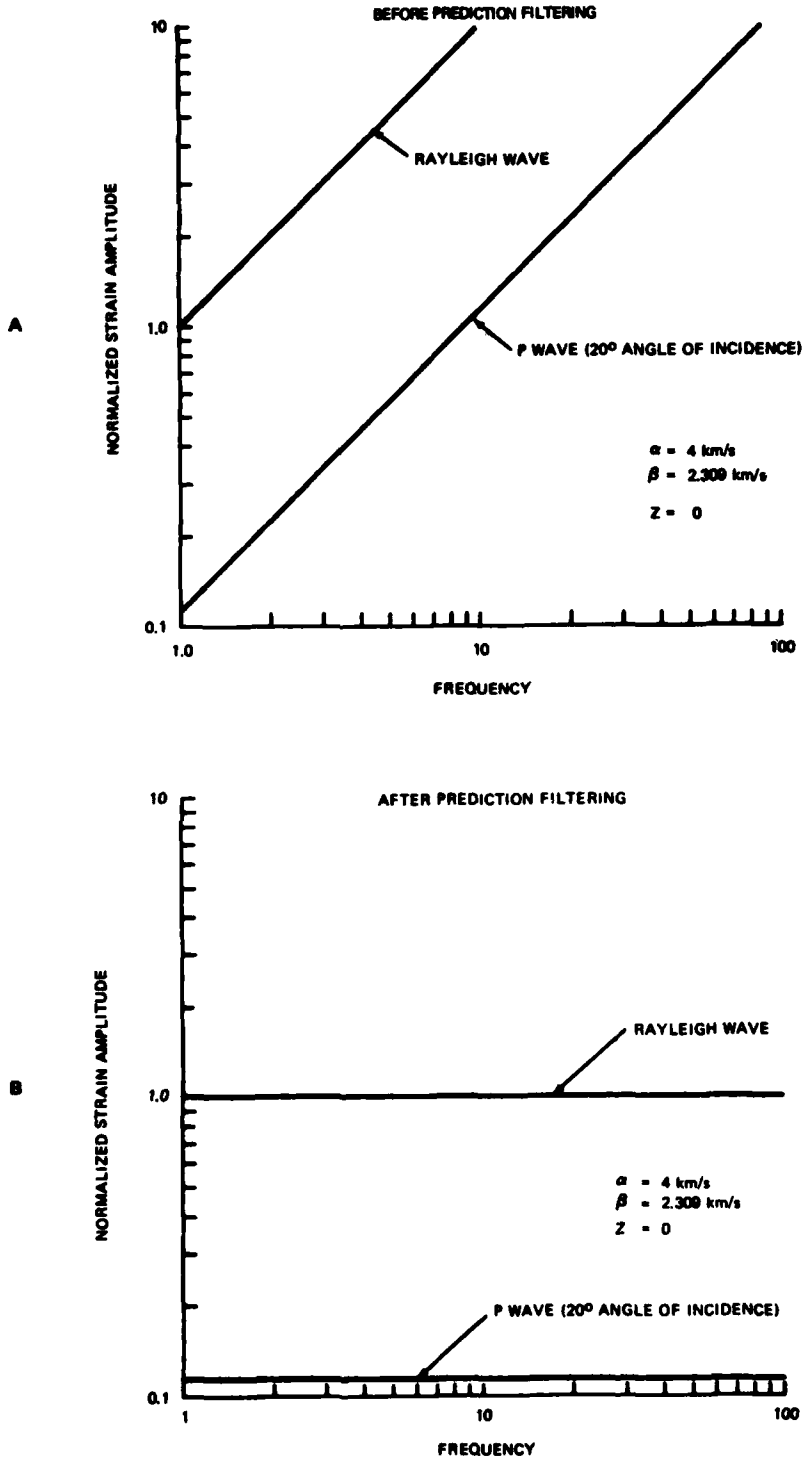

FIGURE 1. NORMALIZED STRAIN-DISPLACEMENT RESPONSE RATIOS

G10740

2.2 CONCEPTUAL NOISE MODELS

Realistic assessment of the SNR enhancement capabilities of S-I systems requires quantitative information regarding the frequency wave number structure and composition of the earth noise in the regional signal bandwidth. Unfortunately, a review of the existing data base earth noise (see section 6) has revealed that this type of information is generally lacking, particularly in the regional signal bandwidth. Thus we must resort to generalized conceptual models of the earth noise in order to obtain a preliminary assessment of the SNR enhancement capabilities of S-I systems. For the purposes of this investigation we shall confine our attention to propagating earth noise fields which consist of both scattered Rayleigh waves and P waves. We shall assume that these fields are laterally homogeneous and time stationary. In addition, the effects of locally generated wind noise and strain system noise will be evaluated under special circumstances. Specific cases examined during the course of this investigation are listed in table 1. It will be noted that SNR enhancement and noise rejection capabilities are considered separately. This is because the relationship between SNR enhancement and noise rejection is generally complicated by the presence of the signal distortion term referred to earlier.

For the purposes of this project we have also limited ourselves to the case where the observation point is located at the surface of a homogeneous, isotropic, elastic half space. While this assumption influences the details of our calculations it has little impact upon the general nature of our results. Furthermore, the current experimental data base concerning earth noise does not justify the use of more sophisticated earth models.

2.3 PREDICTION ERROR FILTER DESIGN

For the remainder of this discussion let us focus our attention upon the potential noise reduction and SNR enhancement capabilities of a linear combination of the outputs of a vertical inertial and vertical strain sensor. Let $n_e(t)$ and $n_i(t)$ be the outputs of the strain and inertial sensors, respectively, when only noise is present. We wish to apply a filter to the output of the strain sensor such that it is the optimum predictor of the noise observed at the output of the inertial sensor in the sense that the mean square difference between the observed and predicted inertial outputs is minimized. If $H(\omega)$ is the complex frequency response of this filter then

$$H(\omega) = \frac{\phi^n_{ei}(\omega)}{\phi^n_{ee}(\omega)} \qquad (1)$$

where $\phi^n_{ei}(\omega)$ is the crosspower spectral relating the strain and inertial outputs and $\phi^n_{ee}(\omega)$ is the power spectral density of the strain output (For readers who are unfamiliar with two channel prediction error operators, eq. 1 is derived in detail in section 1 of the Appendix).

It is convenient for our purposes to define the power and crosspower spectral density functions in terms of their frequency wave number spectra. Thus,

Table 1. Strain-inertial test cases

1. Noise rejection capabilities
   - Rayleigh wave noise contaminated by strain "system" noise
   - Rayleigh wave noise contaminated by "wind" noise
   - Rayleigh wave noise contaminated by "mantle" P wave noise
2. SNR enhancement capabilities
   - Scattered Rayleigh wave noise
   - Scattered P wave noise

$$\phi^{n}_{ei}(\omega,\Delta\vec{r}) = \frac{1}{4\pi^2}\int_{\kappa} N_{ei}\ (\omega,\vec{k})\ \exp\ (-j\vec{k}\cdot\vec{\delta r})\, d\vec{k} \qquad (2)$$

where $N_{ei}\ (\omega,\vec{k})$ is the 3 dimensional crosspower spectral density function, $\vec{k}$ is the vector horizontal wave number, $\delta\vec{r}$ is the vector distance between the strain and inertial observation points and the operation

$$\int_{\kappa} \cdot\ \cdot\ \cdot\ \cdot\ \cdot\ \cdot\ d\vec{k} \qquad (3)$$

indicates an integration over the entire $\vec{k}$ plane. Similarly, if $N_{ee}\ (\omega,\vec{k})$ and $N_{ii}\ (\omega,\vec{k})$ are the 3 dimensional power spectral density functions characterizing the vertical strain and inertial noise fields, then

$$\phi^{n}_{ee}\ (\omega,\Delta\vec{r}) = \frac{1}{4\pi^2}\int_{\kappa} N_{ee}\ (\omega,\vec{k})\ \exp(-j\vec{k}\cdot\vec{\delta r})\ d\vec{k} \qquad (4)$$

and

$$\phi^{n}_{ii}\ (\omega,\Delta\vec{r}) = \frac{1}{4\pi^2}\int_{\kappa} N_{ii}\ (\omega,\vec{k})\ \exp(-j\vec{k}\cdot\vec{\delta r})\ d\vec{k} \qquad (5)$$

2.3.1 Rayleigh Wave Noise Prediction Filters

Let $M_e\ (\omega)$ and $M_i\ (\omega)$ be the complex frequency responses of the strain and inertial sensors. If the propagating earth noise field consists entirely of single mode Rayleigh waves from remote sources then using the results of section 4.2 in the Appendix it can be shown that

$$\phi^{n}_{ei} = |\overline{L}|^2\ M^{*}_{i}\ G^{*}\ M_e\ \frac{\partial G}{\partial Z}\ J_o\ (\kappa_r \delta r) \qquad (6)$$

where $J_o\ (\kappa_r\delta r)$ is a Bessel function of order 0, $|\overline{L}|^2$ is related to the distribution and spectral intensity of the sources and G^{*} and $\frac{\partial G}{\partial Z}$ are the displacement and strain medium response functions. Similarly ϕ^{n}_{ee} and ϕ^{n}_{ii} are defined by

$$\phi^{n}_{ee} = |L|^2 |Me|^2 \left|\frac{\partial G}{\partial Z}\right|^2 \qquad (7)$$

$$\phi^{n}_{ii} = |L|^2 |M_i|^2 |G|^2 \qquad (8)$$

Therefore from equations 1, 6, and 7

$$H(\omega) = \frac{M^{*}_{i}\ Me}{|Me|^2}\ \frac{G^{*}\ \frac{\partial G}{\partial Z}}{\left|\frac{\partial G}{\partial Z}\right|^2}\ J_o\ (k\delta r) \qquad (9)$$

It is important to note that in this case when strain and inertial sensors are colocated, $H(\omega)$ is independent of the intensity and distribution of sources and the state of organization of the corresponding Rayleigh wave fields. This means in effect then that when the earth noise consists solely of unimodal Rayleigh waves the noise prediction filter is dependent only on the strain and displacement medium response functions and frequency response functions of the filters. Since the parameters which determine these functions

are time invariant, the Rayleigh noise prediction filter also shares this property. In the special case where the strain and inertial sensors are colocated at the surface of a homogeneous and isotropic halfspace the medium response functions are defined by equations 3.3.5 in section 3 of the Appendix and H(w) reduces to

$$H(\omega) = \frac{M_i^* M_e}{|M_e|^2} \left\{ \frac{c_r}{[1-\left(\frac{c_r}{\alpha}\right)^2]^{1/2} [2\left(\frac{\beta}{Cr}\right)^2 - 1] - [1-\left(\frac{c_r}{\beta}\right)^2]^{1/2} \left(\frac{\beta}{Cr}\right)^2} \right\} \frac{1}{\omega} \quad (10)$$

where c_r is the Rayleigh wave speed. If we assume that $\lambda = \mu$ then $\alpha = 3\sqrt{\beta}$ and $c_r = 0.9194\beta$ and

$$H(\omega) = \frac{M_i^* M_e}{|M_e|^2} \left\{ \frac{2.337\alpha}{\omega} \right\} \quad (11)$$

The term in brackets is plotted in figure 2 for the case where $\alpha = 4.0$ km/s.

2.3.2 P Wave Noise Prediction Filters

Let us now assume that the propagating noise field consists entirely of scattered P waves with apparent horizontal velocities c distributed in the internal $c_{min} \leq c \leq \alpha$ where

$$c_{min} > \alpha \quad (12)$$

Using the 3 dimensional power and cross power spectral density functions given in section 4.1 of the Appendix, in equations 2, 4 and 5 it is found that

$$\phi_{ei}^n(\omega, \vec{\delta r}) = \frac{M_e^* M_i}{4\pi^2} \int_0^b \int_0^{2\pi} A_1(\theta,\omega) \frac{\partial D^*}{\partial Z} D \exp(-j\vec{k}.\delta) \, k d\theta dk \quad (13)$$

$$\phi_{ee}^n(\omega, \vec{\delta r}) = \frac{|M_e|^2}{4\pi^2} \int_0^b \int_0^{2\pi} A_1(\theta,\omega) \left|\frac{\partial D}{\partial Z}\right|^2 \exp(-j\vec{k}\cdot\vec{\delta r}) \, k d\theta dk \quad (14)$$

$$\phi_{ii}^n(\omega, \vec{\delta r}) = \frac{|M_i|^2}{4\pi^2} \int_0^b \int_0^{2\pi} A_1(\theta,\omega) |D|^2 \exp(-j\vec{k}\cdot\vec{\delta r}) \, k d\theta dk \quad (15)$$

where $A_1(\theta,\omega)$ is the power spectral density of the displacement potential for the incident P wave field, D is the vertical displacement reflectivity function for incident P waves and $\frac{\partial D}{\partial Z}$ is the vertical strain reflectivity function. In the special case where the strain and inertial sensors are colocated at the surface of a homogeneous, and isotropic half space the results of sections 3 and 4 of the Appendix may be used to show that

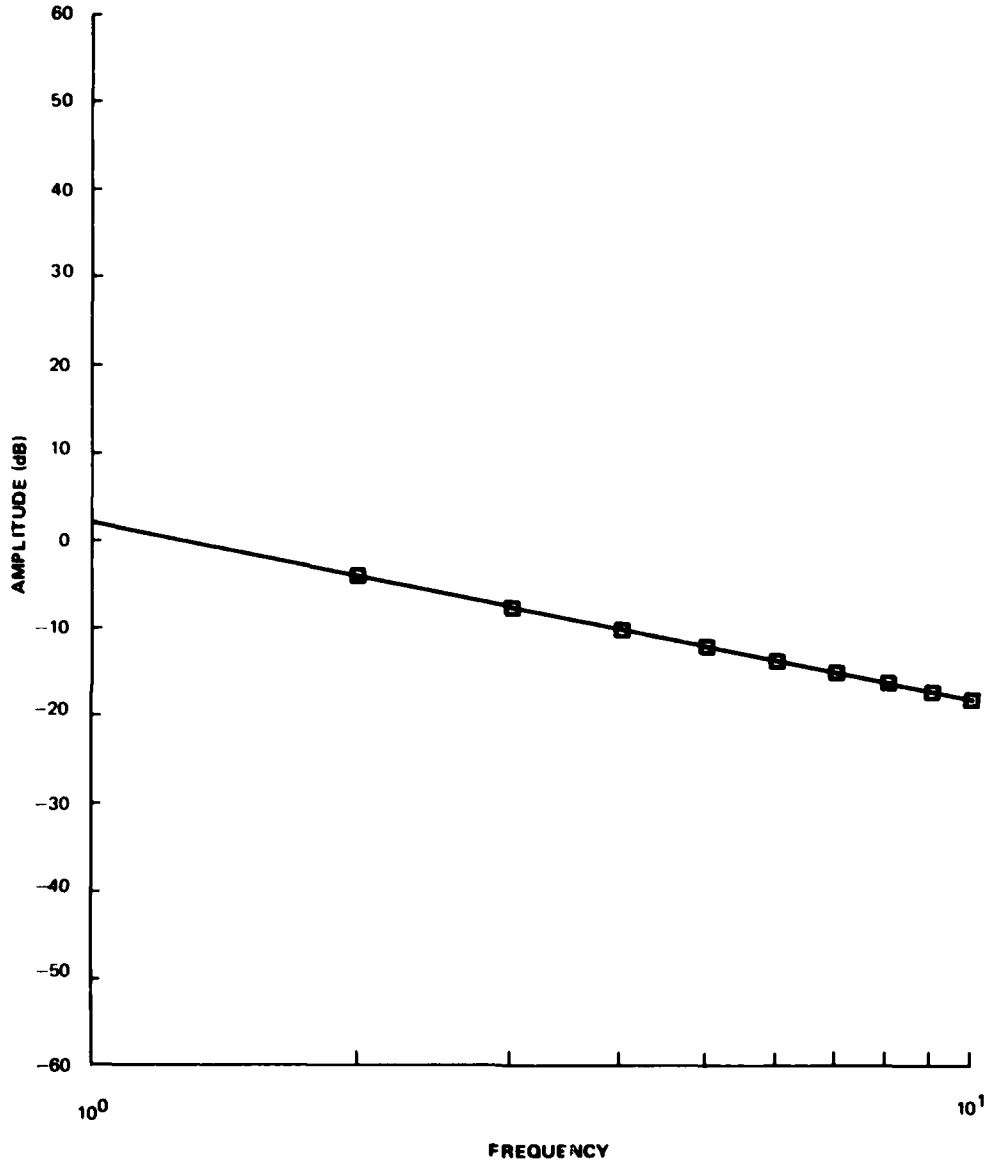

FIGURE 2. MODULUS OF THE FREQUENCY OF A RAYLEIGH WAVE NOISE PREDICTION FILTER. STRAIN AND INERTIAL SENSOR RESPONSES ARE ASSUMED TO BE IDENTICAL.

G 11252

$$D = 2j\left(\frac{\alpha}{\beta}\right)^2 k\alpha \frac{(1-\eta^2)^{1/2}\left(\left(\frac{\alpha}{\beta}\right)^2 - 2\eta^2\right)}{4\eta^2\ (1-\eta^2)^{1/2}\left(\left(\frac{\alpha}{\beta}\right)^2-\eta^2\right)^{1/2}+\left(\left(\frac{\alpha}{\beta}\right)^2-2\eta^2\right)^2} \tag{16}$$

$$\frac{\partial D}{\partial Z} = \frac{4\lambda}{\lambda+2\mu}\ k_\alpha^2 \frac{\eta^2\ (1-\eta^2)^{1/2}\left(\left(\frac{\alpha}{\beta}\right)^2-\eta^2\right)^{1/2}}{4\eta^2\ (1-\eta^2)^{1/2}\left(\left(\frac{\alpha}{\beta}\right)^2-\eta^2\right)^{1/2}+\left(\left(\frac{\alpha}{\beta}\right)^2-2\eta^2\right)^2} \tag{17}$$

where

$$\eta = \sin\theta \tag{18}$$

$$k_\alpha = \frac{\omega}{\alpha} \tag{19}$$

and θ is the angle of incidence for the P wave noise. Given these definitions and assuming that the sensors are colocated equations 13-15 may be written as

$$\phi_{ei}^{n} = -8j\ \frac{M_e^* M_i}{4\pi^2}\ \widetilde{A_1(\omega)}\ \left(\frac{\alpha}{\beta}\right)^2 \frac{\lambda}{\lambda+2\mu}\ k_\alpha^5\ I_{ei}\ (\eta_o) \tag{20}$$

$$\phi_{ee}^{n} = 16|M_e|^2\left(\frac{\lambda}{\lambda+2\mu}\right)^2 \frac{\widetilde{A_1(\omega)}}{4\pi^2}\ k_\alpha^6\ I_{ee}\ (\eta_o) \tag{21}$$

$$\phi_{ii}^{n} = 4|M_i|^2\ \frac{\widetilde{A_1(\omega)}}{4\pi^2}\left(\frac{\alpha}{\beta}\right)^4 k_\alpha^4\ I_{ii}\ (\eta_o) \tag{22}$$

where

$$\widetilde{A_1(\omega)} = \int_0^{2\pi} A_1\ (\theta,\omega)\ d\theta \tag{23}$$

$$I_{ei}\ (\eta_o) = \int_0^{\eta_o} \frac{\eta^2(1-\eta^2)\left(\left(\frac{\alpha}{\beta}\right)^2-2\eta^2\right)\left(\left(\frac{\alpha}{\beta}\right)^2-\eta^2\right)^{1/2}}{F(\eta)}\ \eta d\eta \tag{24}$$

$$I_{ee}\ (\eta_o) = \int_0^{\eta_o} \frac{\eta^4(1-\eta^2)\left(\left(\frac{\alpha}{\beta}\right)^2-\eta^2\right)}{F(\eta)}\ \eta d\eta \tag{25}$$

$$I_{ii}\ (\eta_o) = \int_0^{\eta_o} \frac{(1-\eta^2)\left(\left(\frac{\alpha}{\beta}\right)^2-\eta^2\right)^2}{F(\eta)}\ \eta d\eta \tag{26}$$

and

$$F(\eta) = \left\{4\eta^2(1-\eta^2)^{1/2}\left(\left(\frac{\alpha}{\beta}\right)^2-\eta^2\right)^{1/2}+\left(\left(\frac{\alpha}{\beta}\right)^2-2\eta^2\right)^2\right\}^2 \tag{27}$$

Therefore

$$H(\omega) = -\frac{jM_e^* M_i}{|M_e|^2}\left\{\frac{1}{2}\left(\frac{\alpha}{\beta}\right)^2\left(\frac{\lambda+2\mu}{\lambda}\right)\frac{1}{k\alpha}\right\}\frac{I_{ei}\ (\eta_o)}{I_{ee}\ (\eta_o)} \tag{28}$$

Observe that in this case the noise prediction filter is independent of the azimuthal distribution of the P wave field but is functionally dependent on η_o. Now η_o is related to c_{min} through

$$c_{min} = \frac{\alpha}{\eta_o} \tag{29}$$

Thus the range of apparent horizontal phase velocities for the scattered P waves contained in the field is given by

$$\frac{\alpha}{\eta_o} \leq c \leq \infty \tag{30}$$

$|H(\omega)|$ for representative values of η_o are plotted in figure 3 for the case where $M_e=M_i$, $\lambda=\mu$, and $\alpha=4.0$ km/sec. Notice that the gain of the frequency response functions diminish as η_o increases. In other words, in a P wave noise field, the shape and phase of the noise prediction filter response are constants but the gain will change in response to changes in the range of apparent horizontal velocities contained in the field.

2.3.3 Prediction Filters for Multicomponent Noise Fields

Let us consider the case where the outputs of the strain and inertial sensors contains two statistically independent components, i.e.;

$$n_e(t) = n_{e1}(t) + n_{e2}(t) \tag{31}$$

$$n_i(t) = n_{i1}(t) + n_{i2}(t) \tag{32}$$

Then

$$\phi^{n}_{ei}(\omega) = \phi^{1}_{ei}(\omega) + \phi^{2}_{ei}(\omega) \tag{33}$$

and

$$\phi^{n}_{ee}(\omega) = \phi^{1}_{ee}(\omega) + \phi^{2}_{ee}(\omega) \tag{34}$$

where ϕ^{1}_{ei} and ϕ^{2}_{ei} are crosspower spectral densities relating the strain and inertial outputs for components 1 and 2 and $\phi^{1}_{ee}(\omega) + \phi^{2}_{ee}(\omega)$ are the strain power spectral density functions. Therefore,

$$H(\omega) = \frac{\phi^{1}_{ei} + \phi^{2}_{ei}}{\phi^{1}_{ee} + \phi^{2}_{ee}}$$

$$= B_1 H_1(\omega) + B_2 H_2(\omega) \tag{35}$$

where

$$H_1(\omega) = \frac{\phi^{1}_{ei}}{\phi^{1}_{ee}}, \tag{36}$$

$$H_2(\omega) = \frac{\phi^{2}_{ei}}{\phi^{2}_{ee}} \tag{37}$$

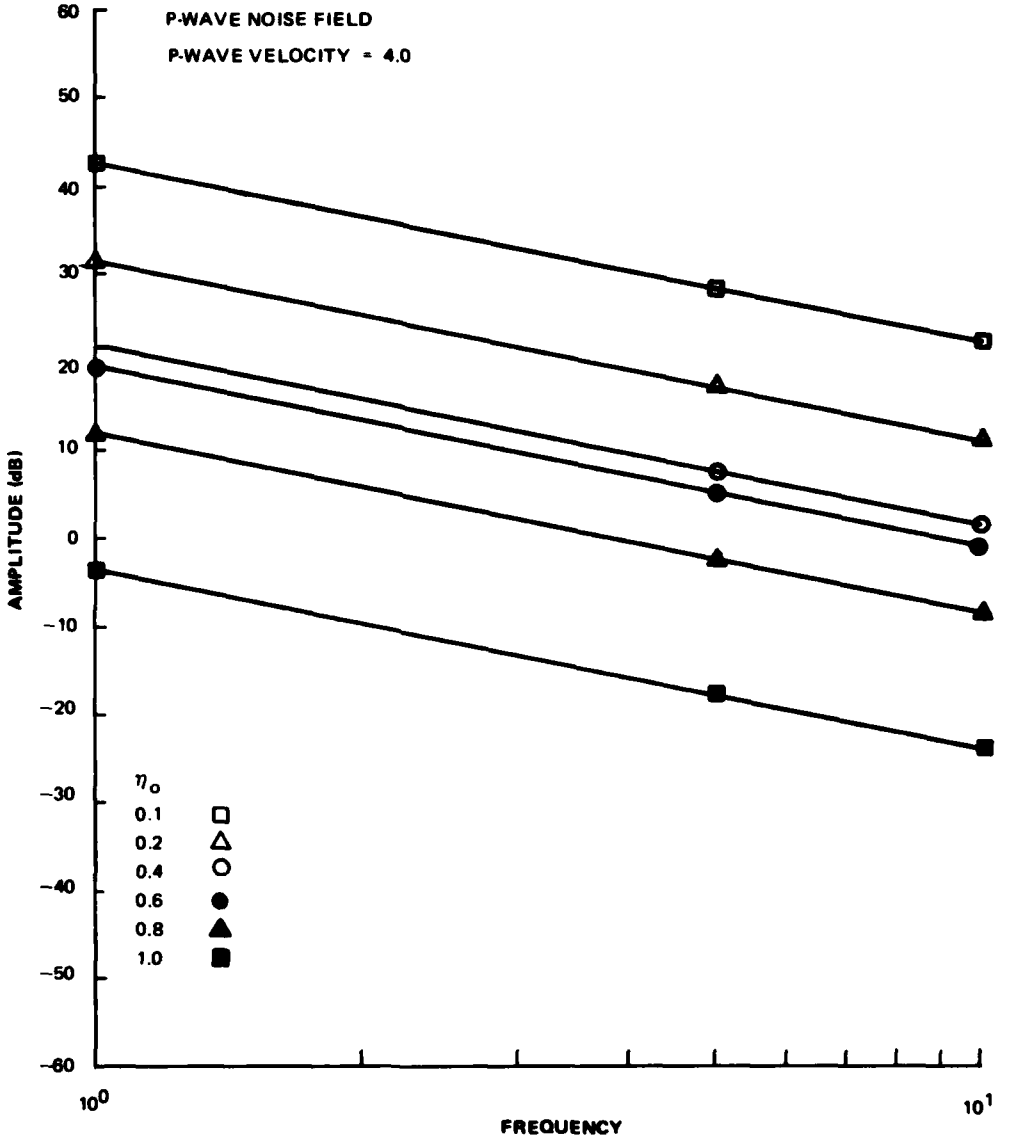

FIGURE 3. MODULUS OF THE FREQUENCY RESPONSE OF A P-WAVE NOISE PREDICTION FILTER. STRAIN AND INERTIAL SENSOR RESPONSES ARE ASSUMED TO BE IDENTICAL

G 11253

are the optimum frequency response functions that would apply for fields consisting solely of component 1 or component 2 and

$$B_1 = \frac{\phi^1_{ee}}{\phi_{ee}} \quad , \tag{38}$$

$$B_2 = \frac{\phi^2_{ee}}{\phi_{ee}} \tag{39}$$

are the ratios of the power in components 1 and 2 relative to the total noise power observed at the output of the strain sensor. By analogy, then if the noise field consists say ℓ statistically independent components

$$H(\omega) = \sum_{\ell=1}^{L} B_\ell \, H_\ell \, (\omega) \tag{40}$$

That is, the optimum noise prediction filter for a multicomponent field is the weighted sum of the optimum prediction filters for the individual components where the weights are the fractional noise power in each component.

Now suppose one of the components is strain system noise, then for the case of the two component noise field

$$H(\omega) = B_1 \, H_1 \, (\omega) = (1-B_s) \, H_1 \, (\omega) \tag{41}$$

since the strain system noise has no counter part at the output of the inertial sensor. Thus the gain of the optimum filter will decrease as the percentage of system noise in the total strain noise increases.

2.4 NOISE REDUCTION

Let $\hat{\phi}_{ii}$ be the power spectral density of the output of the noise prediction filter. It follows from the previous discussion that

$$\hat{\phi}_{ii} = |H^2| \, \phi_{ee} \tag{42}$$

Let γ^2_{ei} be the ratio of predicted inertial noise power to the actual inertial noise power. Then

$$\gamma^2_{ei} = \frac{\hat{\phi}_{ii}}{\phi_{ii}}$$

$$= \frac{|H|^2 \phi_{ee}}{\phi_{ii}}$$

$$= \frac{|\phi_{ei}|^2}{\phi_{ee}\phi_{ii}} \tag{43}$$

The term on the RHS of equation 43 is recognized as the square of the simple coherence relating the strain and inertial outputs. Now it is shown in section 1 of the Appendix that the power spectral density of the noise remaining

after subtracting the predicted from the observed inertial output is given by

$$N = \phi^n_{ii} \ (1-\gamma^2_{ei}) \tag{44}$$

The ratio of the noise power remaining after prediction error filter to the observed inertial noise power is therefore

$$R = \frac{N}{\phi^n_{ii}} = 1-\gamma^2_{ei} \tag{45}$$

R measures the noise reducing capabilities of the prediction error filtering process. In the following paragraphs we shall investigate the behavior of R under various seismic noise conditions.

2.4.1 Rayleigh Waves Contaminated by Strain System Noise

It is shown in section 5.1 of the Appendix that if the earth noise consists entirely of Rayleigh waves of the same mode then

$$R \approx B \tag{46}$$

where B is the ratio of system noise power to total noise power observed at the output of the strain sensor. It is important to notice that in this case the noise reducing capabilities are inherently broad band and limited only by the presence of system noise. Clearly if strain system noise levels can be maintained at relatively low levels then a linear combination of vertical strain and inertial transducers can be a powerful tool for reducing Rayleigh wave noise.

2.4.2 Rayleigh Waves Contaminated by Wind Noise

Earth movement in response to wind generated atmospheric pressure changes is a common constituent of the earth noise observed at many surface locations. It is worthwhile therefore to determine its impact on the noise reducing capabilities of a vertically oriented S-I system. It is shown in section 5.2 of the Appendix that in this instance

$$R = \frac{\left(1-\frac{Q}{T}\right)^2 B(1-B)}{\left(1-\frac{Q}{T}\right)^2 B(1-B) + \left[1-\left(1-\frac{Q}{T}\right)B\right]^2} \tag{47}$$

where B is the ratio of the wind noise power to the total noise power at the output of the strain sensor and Q^{-1} and T^{-1} are the moduli of the strain-displacement response ratios for the wind noise and Rayleigh wave noise components respectively. It is also shown in section 5.2 that if the observation point is at the surface of a homogeneous and isotropic half space then $\frac{Q}{T}$ is of the order of 10^{-3} and that

$$R \approx B \ , \ B \not\approx 1 \tag{48}$$

Equation 47 has been evaluated explicitly for the case where $\lambda=\mu$, $\alpha=4.0$ km/s and the wind speed is 10 meters/s. The results are shown in figure 4. Observe that the linear relationship between R and B persists throughout almost

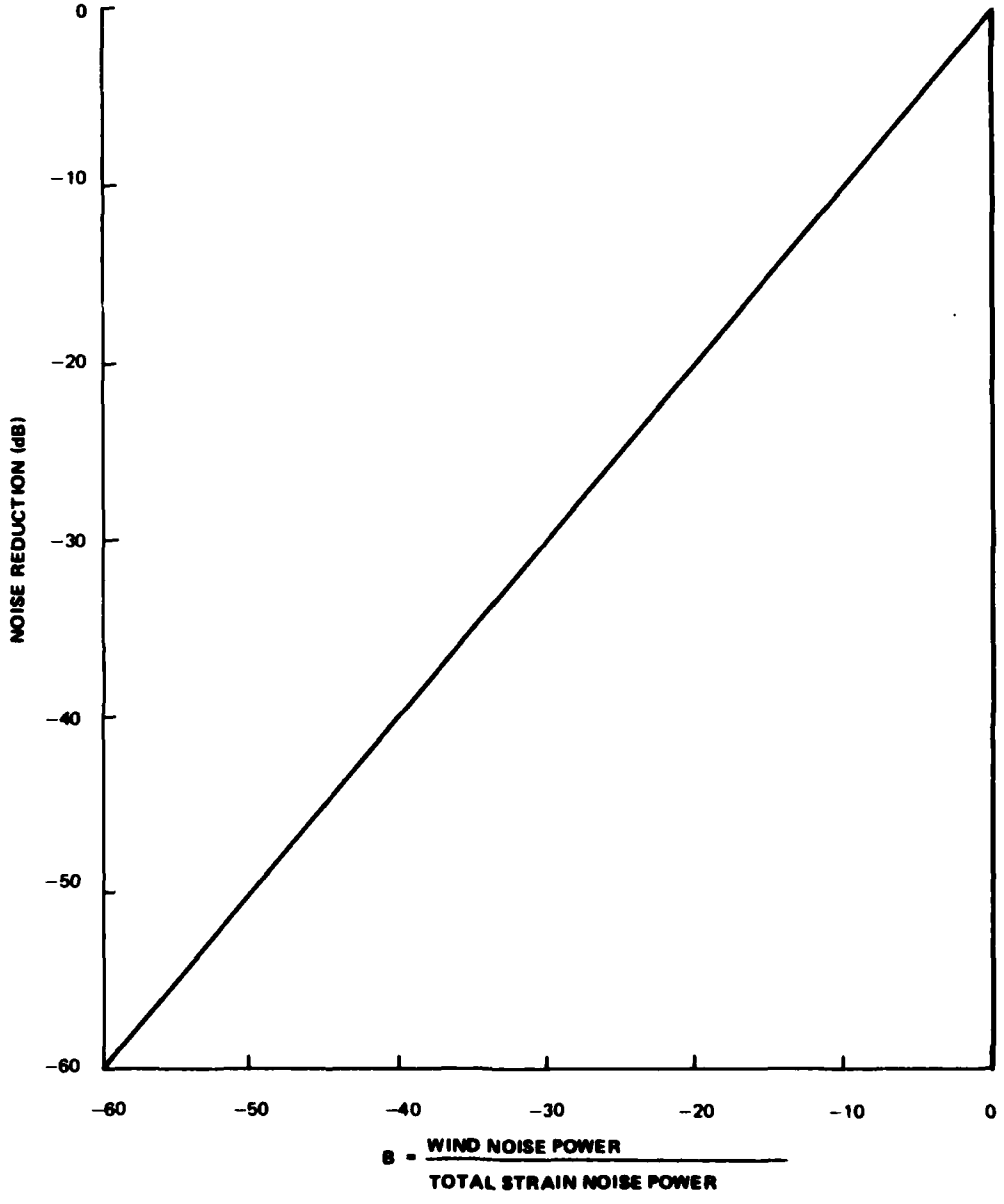

FIGURE 4. THE THEORETICAL EFFECTS OF "WIND" NOISE CONTAMINATION ON THE NOISE REDUCING CAPABILITIES OF AN S-I SYSTEM

G 11254

the entire range of B. Actually it is shown in section 5.2 of the Appendix that R will decrease as B increases only for values of $B \geq \frac{1}{1+\frac{Q}{T}}$.

Thus far, all practical purposes, equation 48 adequately described the noise reducing capabilities of a vertically oriented S-I system in a field consisting of Rayleigh waves and wind noise. Observe that equations 46 and 48 are identical. This means in effect, that wind noise contamination is equivalent to strain system noise contamination insofar as its impact on the noise reduction capabilities of the vertically oriented S-I system is concerned. This is an important result and implies that the design of the system installation to suppress wind noise is equivalent in importance to the design of sensors to suppress system noise.

Equation 48 is not inherently limited to fields consisting only of Rayleigh wave noise and wind noise. It could for example apply to a field consisting of two scattered Rayleigh modes provided that Q^{-1} and T^{-1} specify their vertical strain-displacement response ratios. To illustrate the impact of model interference we have evaluated equation 47 for the cases where $\frac{Q}{T}$ was arbitrarily assigned the value 0.5. The results are shown in figure 5. The important features to note are that R always has a maximum somewhere in the interval $0<B<1$ and vanishes at the end points of this range. It is shown in section 5.2 of the Appendix that the maximum occurs at

$$B = \frac{1}{1+\frac{Q}{T}} \tag{49}$$

and that its value at that point is given by

$$R_{max} = \left(\frac{1-\frac{Q}{T}}{1+\frac{Q}{T}}\right)^2 \tag{50}$$

Equations 49 and 50 show that as $\frac{Q}{T} \to 1$ the maximum occurs at successively smaller values of B and diminishes in magnitude. Thus the noise reduction capabilities of a strain inertial system can vary substantially depending upon the strain-displacement responsibilities for the interfering modes and their power with respect to the total power at the output of the strain sensor.

2.4.3 Rayleigh Waves Contaminated by Mantle P Waves

P waves arriving at near vertical angles of incidence are believed to be a significant constituent of the earth noise at frequencies greater than about 0.5 to 2.0 Hz. This component is commonly referred to as "mantle P wave" noise. It is important to assess the effects that the presence of a mantle P wave component has on the noise reducing capabilities of a vertically oriented S-I system. For our purposes it will be convenient to express the noise reduction R in terms of the ratio of the mantle P wave noise power to the total noise power as observed at the output of the inertial sensor. If B_p is this ratio then it is shown in section 5.3 of the Appendix that

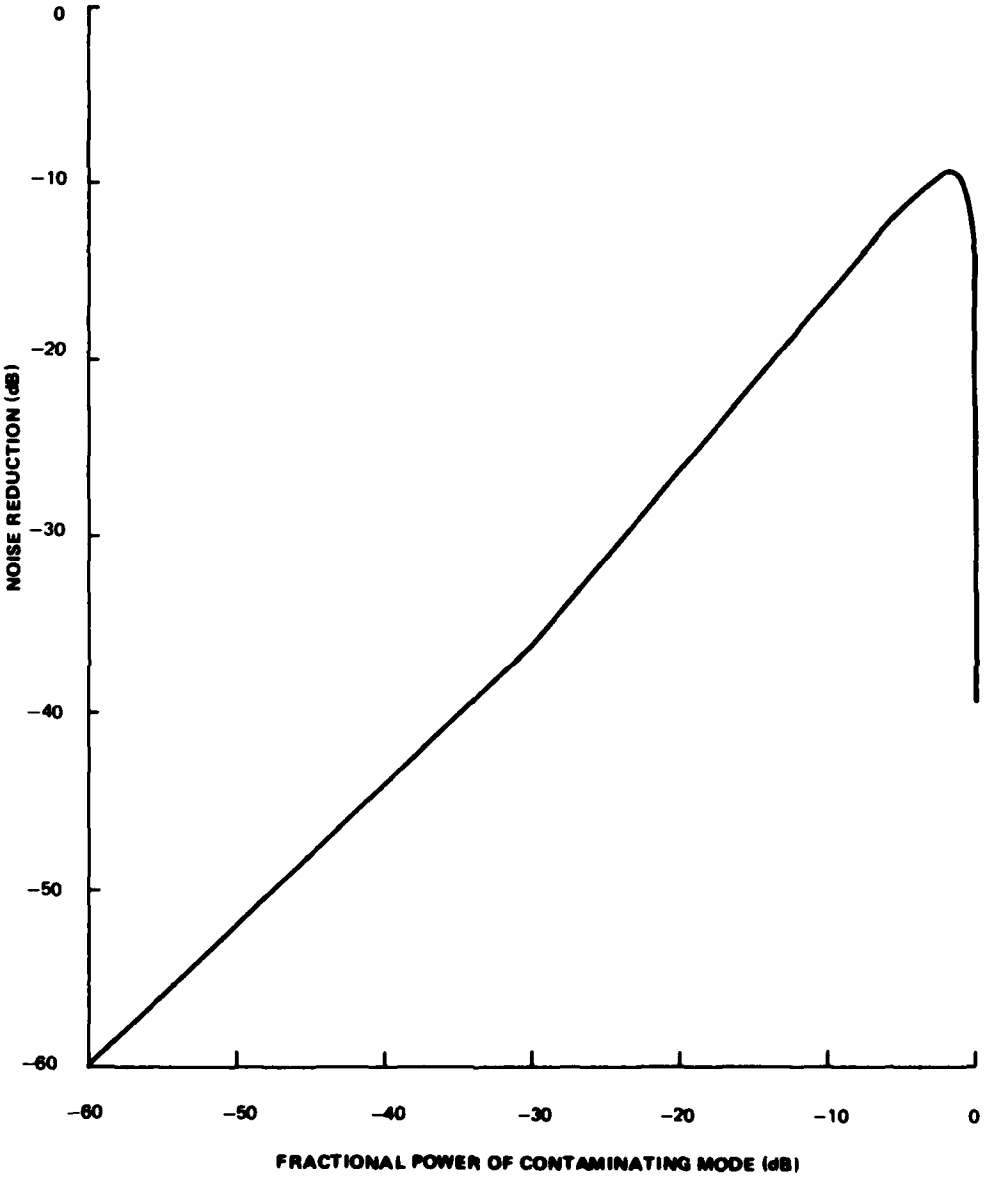

FIGURE 5. THE THEORETICAL EFFECTS OF RAYLEIGH WAVE MODE INTERFERENCE. TWO MODES ARE ASSUMED TO BE PRESENT AND $\frac{Q}{T}$ IS ASSIGNED THE VALUE OF 0.5.

G 11255

$$R = \frac{\left(1 + \left(\frac{P}{V}\right)^2\right) B_p \ (1-B_p)}{1 - \left(1 - \left(\frac{P}{V}\right)^2\right) B_p} \tag{51}$$

where P and V are the moduli of the strain-displacement response ratios for the mantle P wave noise and Rayleigh wave noise, respectively. It is also shown in the same section that if the range of velocities for the scattered waves is small and if the observation point lies at surface of a homogeneous and isotropic half space then $(\frac{P}{V})^2$ is of the order of 10^{-3} and

$$R \approx B_p \quad , \quad B_p \neq 1 \tag{52}$$

Equation 51 has been evaluated explicitly for the case where $\lambda = \mu$, α=4.0 km/sec and the angles of incidence for the incoming P waves lie in a narrow cone centered on 5°. The results are shown in figure 6. Observe that equation 52 is a good approximation to equation 51 for most of the range of B_p. It is shown in section 5.3 that R will begin to deviate significantly from a simple linear dependence on B_p only for values of B_p such that

$$B_p \geq \frac{1}{1+\frac{P}{V}} \tag{53}$$

at this point R reaches a maximum value of

$$R_{max} = \frac{\left[1 + \left(\frac{P}{V}\right)^2\right]}{1 + \frac{P}{V}} \tag{54}$$

and thereafter rapidly declines as $B_p \to 1.0$. These results may be given the following interpretation. In the interval $0 \leq B_p < \frac{1}{1+\frac{P}{V}}$ prediction error filtering will strip away the Rayleigh wave noise leaving the mantle P wave noise as the residual. In the interval $\frac{1}{1+\frac{P}{V}} \leq B_p < 1.0$ prediction error filtering begin to suppress the P wave noise and this suppression will be complete at $B_p \doteq 1$.

2.4.4 Scattered P Wave Noise

In the previous section it was shown that when the background noise consists primarily of P waves arriving in a narrow cone surrounding a near vertical angle of incidence large noise reductions are possible. Let us now consider the limiting case where the noise consists solely of P waves with angles of incidence scattered in the interval $0 < \theta < \theta_o$ where

$$\theta_o = \sin^{-1}\eta_o \tag{55}$$

is the maximum angle of incidence in the field. If the strain and inertial sensors are colocated at the surface of a homogeneous and isotropic elastic half space, then equations 22 and 28 may be used in equation 43 to show that

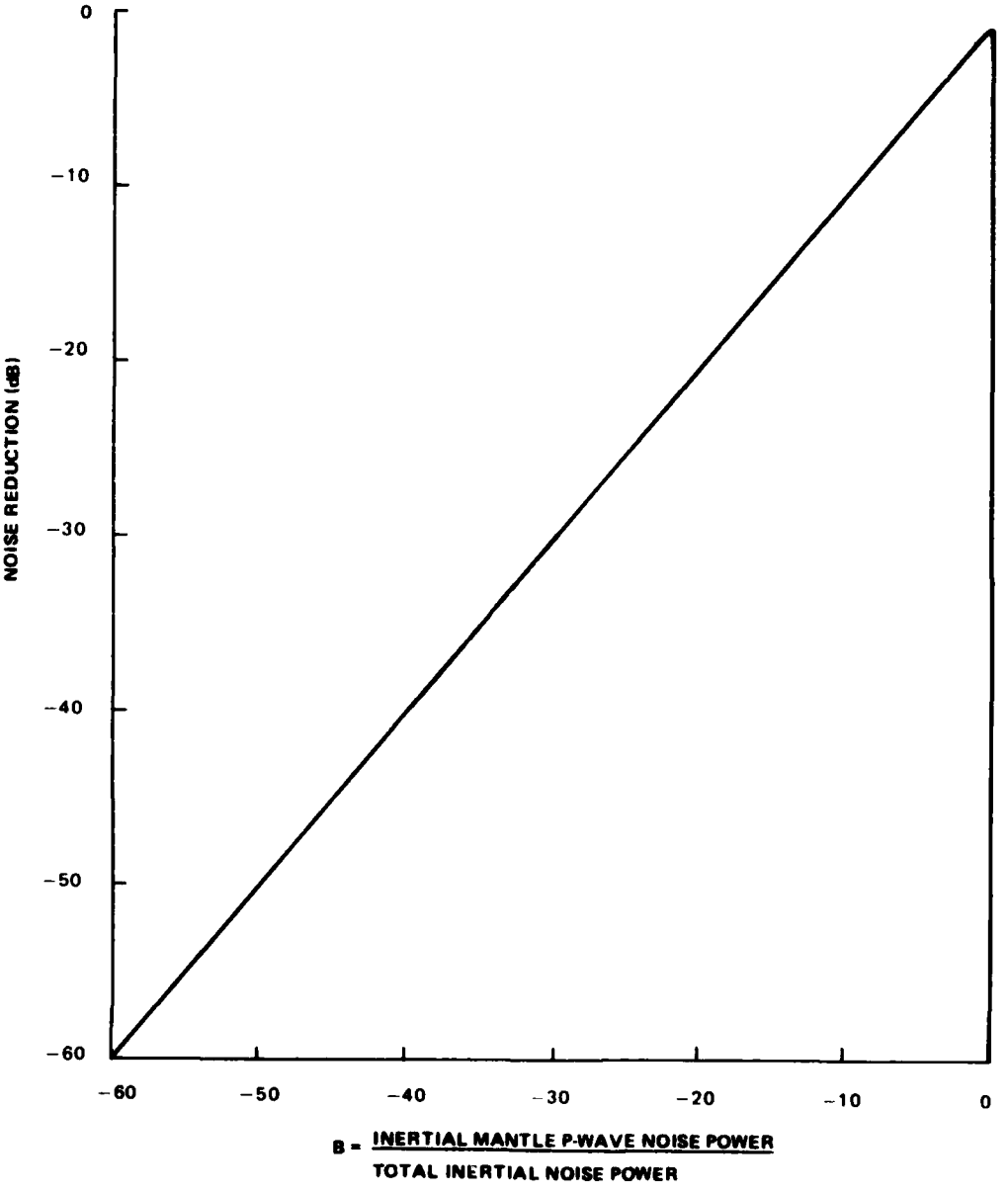

FIGURE 6. THE THEORETICAL EFFECTS OF "MANTLE P-WAVE" NOISE CONTAMINATION ON THE NOISE REDUCING CAPABILITIES OF A S-I SYSTEM

G 11256

$$\gamma_{ei}^2 = \frac{|I_{ei}(\eta_o)|^2}{I_{ee}(\eta_o) I_{ii}(\eta_o)} \tag{56}$$

Therefore using equation 45

$$R = 1 - \frac{|I_{ii}(\eta_o)|^2}{I_{ee}(\eta_o)\, I_{ii}(\eta_o)} \tag{57}$$

Equation 57 shows that for the P wave model under consideration the noise reduction is an implicit function of the maximum angle of incidence for the scattered waves. It has been evaluated for representative values of θ_o for the case where $\lambda=\mu$ and $\alpha=4.0$ km/s. The results are shown in figure 7. Observe that in this instance, prediction error filtering will reduce the noise by about 6-9 dB at the most and then only when the maximum angle of incidence for the waves in the field is 45° or less. For larger maximum angles of incidence the performance of the filtering process rapidly degrades to zero.

2.5 SIGNAL DISTORTION

Let us now consider the case where the outputs of the strain and inertial sensors consist of noise plus signal and let us assume that an optimum noise reducing filter has been designed on the basis of prior information about the noise. It is shown in section 2 of the Appendix that the signal power after prediction error filtering is given by

$$S(\omega) = \phi_{ii}^s \left\{ 1 + |H|^2 \frac{\phi_{ee}^s}{\phi_{ii}^s} - \frac{2\,\mathrm{Re}\,(H^* \phi_{ei}^s)}{\phi_{ii}^s} \right\} \tag{58}$$

where ϕ_{ee}^s and ϕ_{ii}^s are the power spectral densities of the signal at the outputs of the strain and inertial sensors, respectively and ϕ_{ei}^s is the crosspower spectral density between the strain and inertial outputs when only the signal is present. Let $\bar{S}(\omega)$ be the ratio of the signal power after prediction error processing to the signal observed at the output of the inertial sensor. Then

$$\bar{S}(\omega) = \frac{S(\omega)}{\phi_{ii}^s} = 1 + |H|^2 \frac{\phi_{ee}^s}{\phi_{ii}^s} - \frac{2\,\mathrm{Re}\,(H^* \phi_{ei}^s)}{\phi_{ii}^s} \tag{59}$$

$\bar{S}(\omega)$ is thus a measure of the signal distortion power introduced by prediction error filtering. For the purposes of illustration let us assume a plane P wave signal and colocated sensors at the surface of a homogeneous and isotropic half space. Then using the results of section 3 of the Appendix it can be shown that

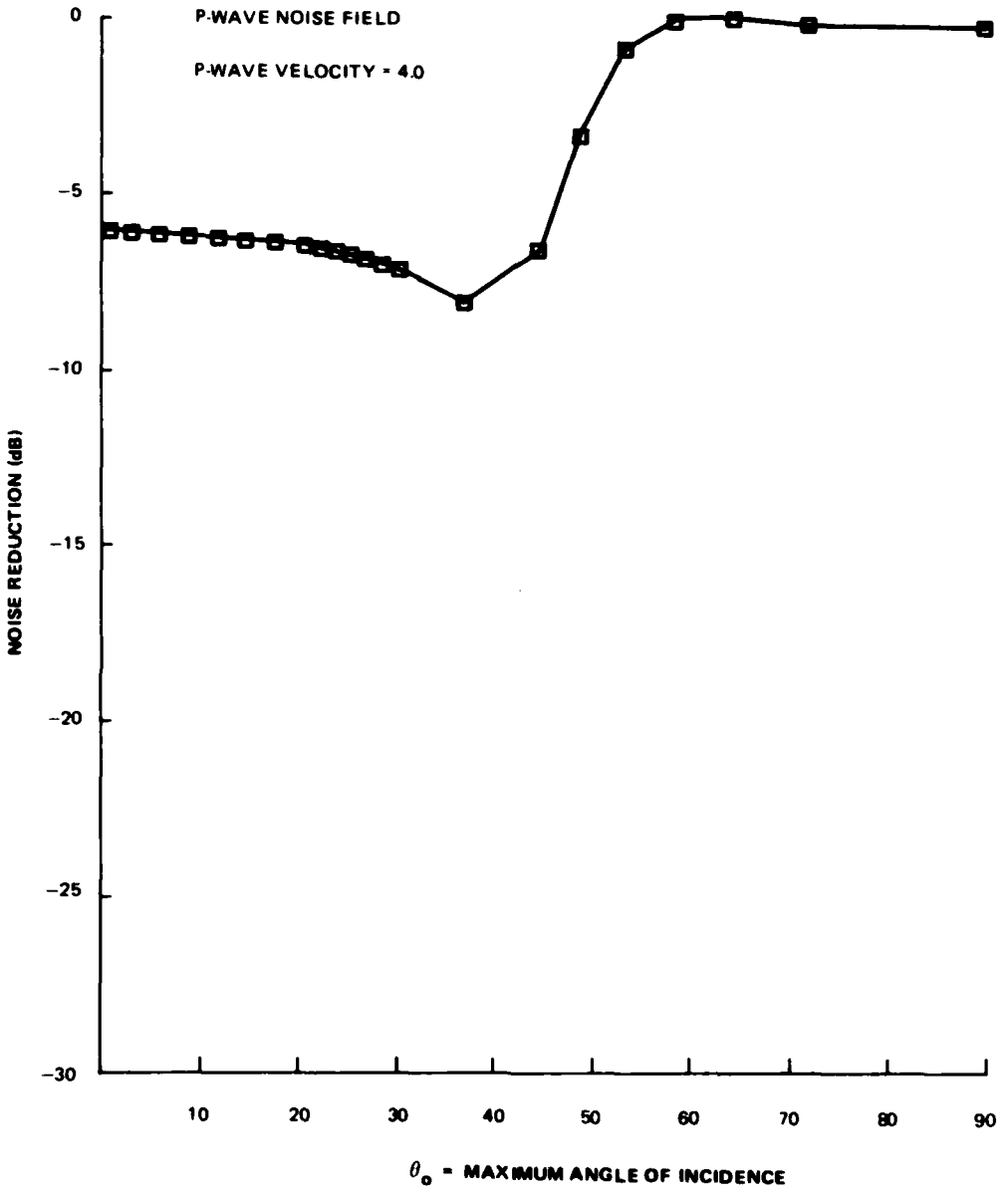

FIGURE 7. THEORETICAL NOISE REDUCING CAPABILITIES OF AN S-I SYSTEM IN P-WAVE NOISE FIELDS WITH DIFFERENT MAXIMUM ANGLES OF INCIDENCE

G 11257

$$\frac{\phi^s_{ee}}{\phi^s_{ii}} = 4 \left(\frac{\lambda}{\lambda+2\mu}\right)^2 \left(\frac{\beta}{\alpha}\right)^4 k_\alpha^2 \frac{\eta_s^4 \left(\left(\frac{\alpha}{\beta}\right)^2 - \eta_s^2\right)}{\left(\left(\frac{\alpha}{\beta}\right)^2 - 2\eta_s^2\right)^2} \tag{60}$$

$$\frac{\phi^s_{ei}}{\phi^s_{ii}} = 2j \left(\frac{\lambda}{\alpha+2\mu}\right) \left(\frac{\beta}{\alpha}\right)^2 k\alpha \frac{\eta_s^2 \left(\frac{\alpha^2}{\beta^2} - \eta_s^2\right)^{1/2}}{\left(\left(\frac{\alpha}{\beta}\right)^2 - 2\eta_s^2\right)} \tag{61}$$

Now let us consider the case of signal distortion caused by prediction error filtering in a Rayleigh wave noise field. It can be seen from equation 10 that in this instance $H(\omega)$ is real while $\frac{\phi^s_{ei}}{\phi^s_{ii}}$ is a pure imaginary. Therefore in this case $\bar{S}(\omega)$ reduces to

$$\bar{S}(\omega) = 1 + H^2 \frac{\phi^s_{ee}}{\phi^s_{ii}} \tag{62}$$

It can be seen from equations 10 and 61 that $S(\bar{\omega})$ is independent of frequency and depends only on the elastic constants of the medium and the angle of incidence of the signal. Equation 62 has been evaluated for the case where α=4.00 km/s for signal angles of incidence in the interval from 0-90°. The results are displayed in figure 8. It is important to note that signal distortion power is for all practical purposes negligible for signals with angles of incidence less than about 45°. Since most regional and teleseismic P wave signal satisfy this constraint, the effects of signal distortion arising from prediction error filtering, if the noise field consists primarily of Rayleigh waves, may be neglected.

Now let us consider the effects of signal distortion when the ambient noise field consists entirely of scattered P waves. In this instance it can be seen from equation 28 that H is a pure imaginary. Hence equation 59 becomes

$$S(\omega) = \left(1 - |H| \frac{|\phi^s_{ei}|}{\phi^s_{ii}}\right)^2 \tag{63}$$

This function is frequency independent but is sensitive to the range of incident angles characterizing the scattered P wave noise field through H and to the incident angle of the signal through the ratio $\frac{|\phi^s_{ei}|}{\phi^s_{ii}}$. Equation 63 has been evaluated for the ranges of noise field incident angles used in section 2.4.4 and for representative signal incident angles in the interval $0 < \theta_s < 90°$. The results for the case where $\lambda = \mu$ and α=4.0 km/s are shown in figure 9. It is important to observe that signal distortion can act to both increase and decrease the signal power observed at the output of the prediction error filter relative to the power observed at the output of the inertial sensor. Generally speaking these curves show that if the angle of incidence for the signal lies outside the range of incident angles for the scattered P wave noise

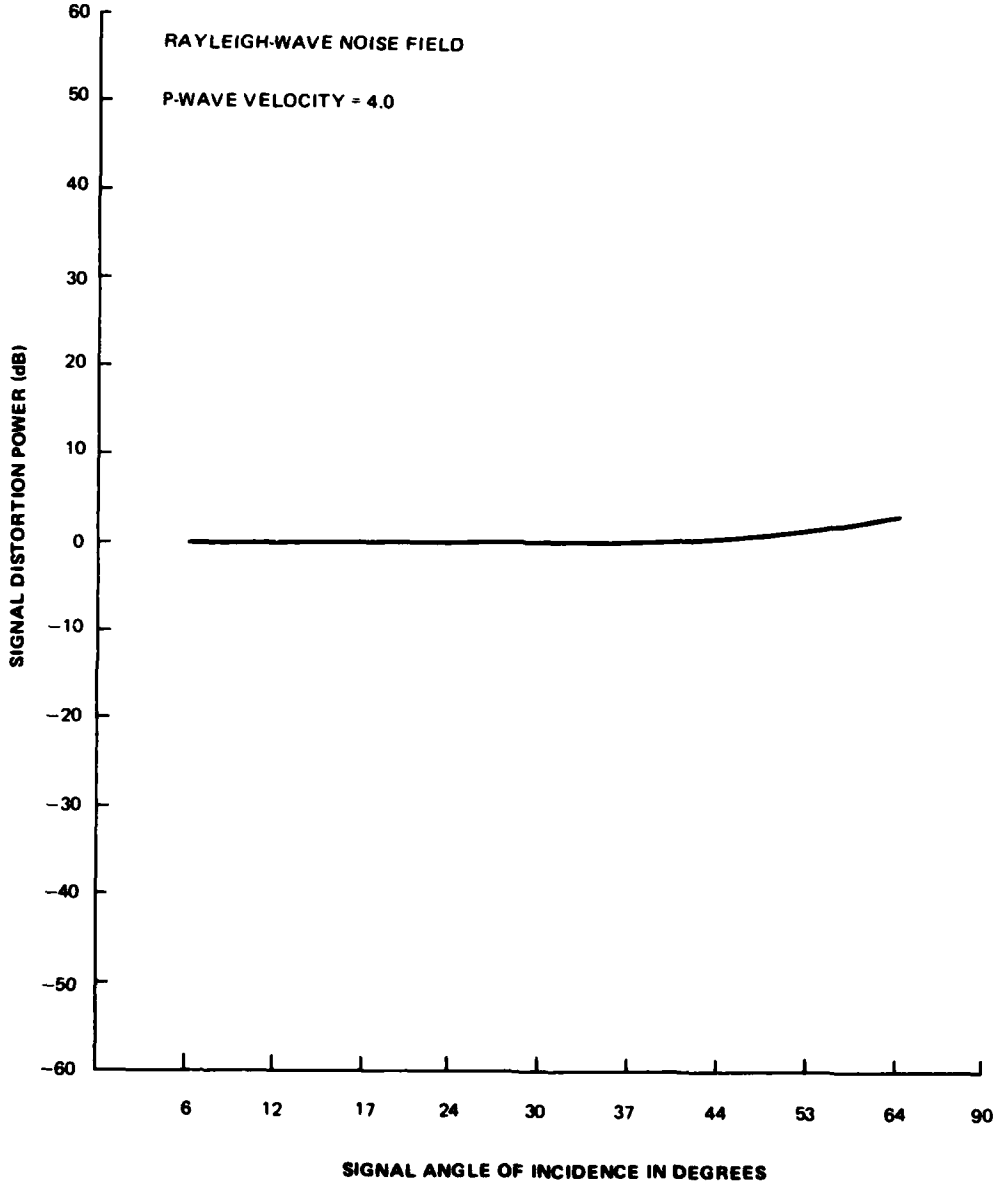

FIGURE 8. THEORETICAL SIGNAL DISTORTION EFFECTS FOR RAYLEIGH-WAVE NOISE PREDICTION

G 11258

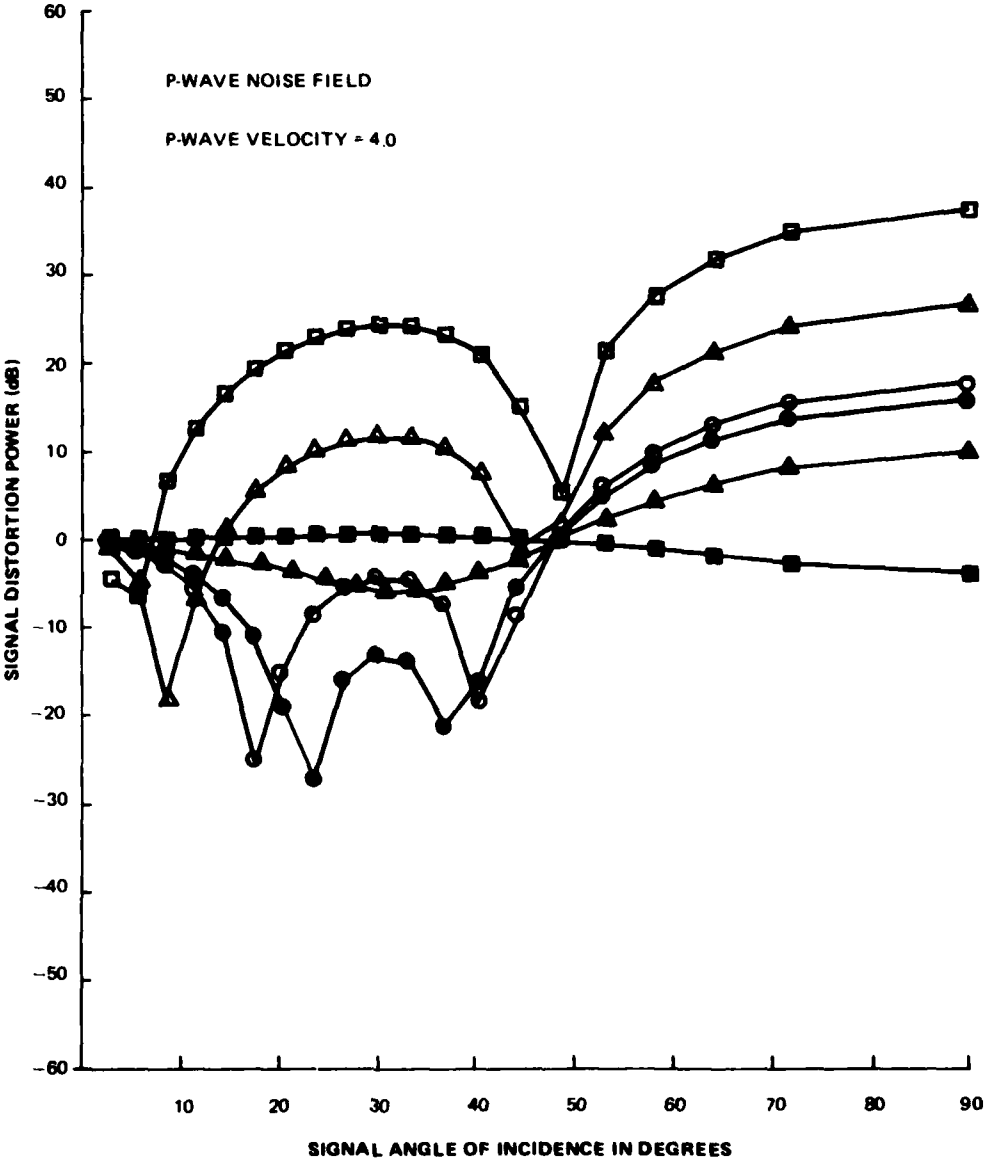

FIGURE 9. THEORETICAL SIGNAL DISTORTION EFFECTS FOR P-WAVE NOISE PREDICTION

G 11259

the signal power will be increased by prediction error filtering. This increase is substantial in those cases where the angles of incidence is less than about 12° and the signal angle of incidence is greater than about 15°. This result suggests that if there are sites where so called mantle P waves are the sole contribution to the noise field, the signal distortion effect could provide significant increases in regional P wave SNRs. As one might expect, when the signal angle of incidence lies within the range of those characterizing the noise, the signal power at the output of the prediction error filter will generally be less than or equal to the power observed at the output of the inertial sensor.

2.6 SNR ENHANCEMENT

Let us define the SNR enhancement, I, as the ratio of the power SNR observed at the output of the prediction error filter to the power SNR observed at the output of the inertial sensor. It then follows from the definitions of the noise reduction, R, and the signal distortion $\bar{S}$, that

$$I = \frac{\bar{S}}{R} \tag{64}$$

Let us first consider the case of Rayleigh wave noise contaminated by strain system noise. Utilizing the results presented in sections 2.4 and 2.5 we obtain the curve shown in figure 10 where SNR enhancement is plotted as a unction of signal angle of incidence. In this particular example, B, the ratio of system noise power to total noise power at the output of the strain sensor, was chosen to be 0.01. We know from our previous discussion that the effects of signal distortion may be safely neglected for most regional and teleseismic P waves and that R = B. Therefore, for all practical purposes

$$I \simeq \frac{1}{B} \tag{65}$$

In other words, P wave signal enhancement in a Rayleigh wave noise field is totally controlled by the strain system noise power.

We also know from the results of section 2.4.2 that if the Rayleigh wave field is contaminated by wind noise then R B, where, in this instance B is the ratio of wind noise power to total noise power observed at the output of the strain sensor. Thus the curve shown in figure 10 is equally representation of the SNR enhancement obtained in a noise field whose power is 99% Rayleigh waves and 1% wind noise. Furthermore, it is clear that equation 65 also approximately describes the SNR enhancement that prediction error filtering will provide in these types of field. More generally it can be inferred from this discussion that if B_s and B_w are the ratios of the system noise and wind noise powers to the total noise observed at the output of the strain sensor, then the SNR enhancement can be written approximately as

$$I \simeq \frac{1}{B_s + B_w} \tag{66}$$

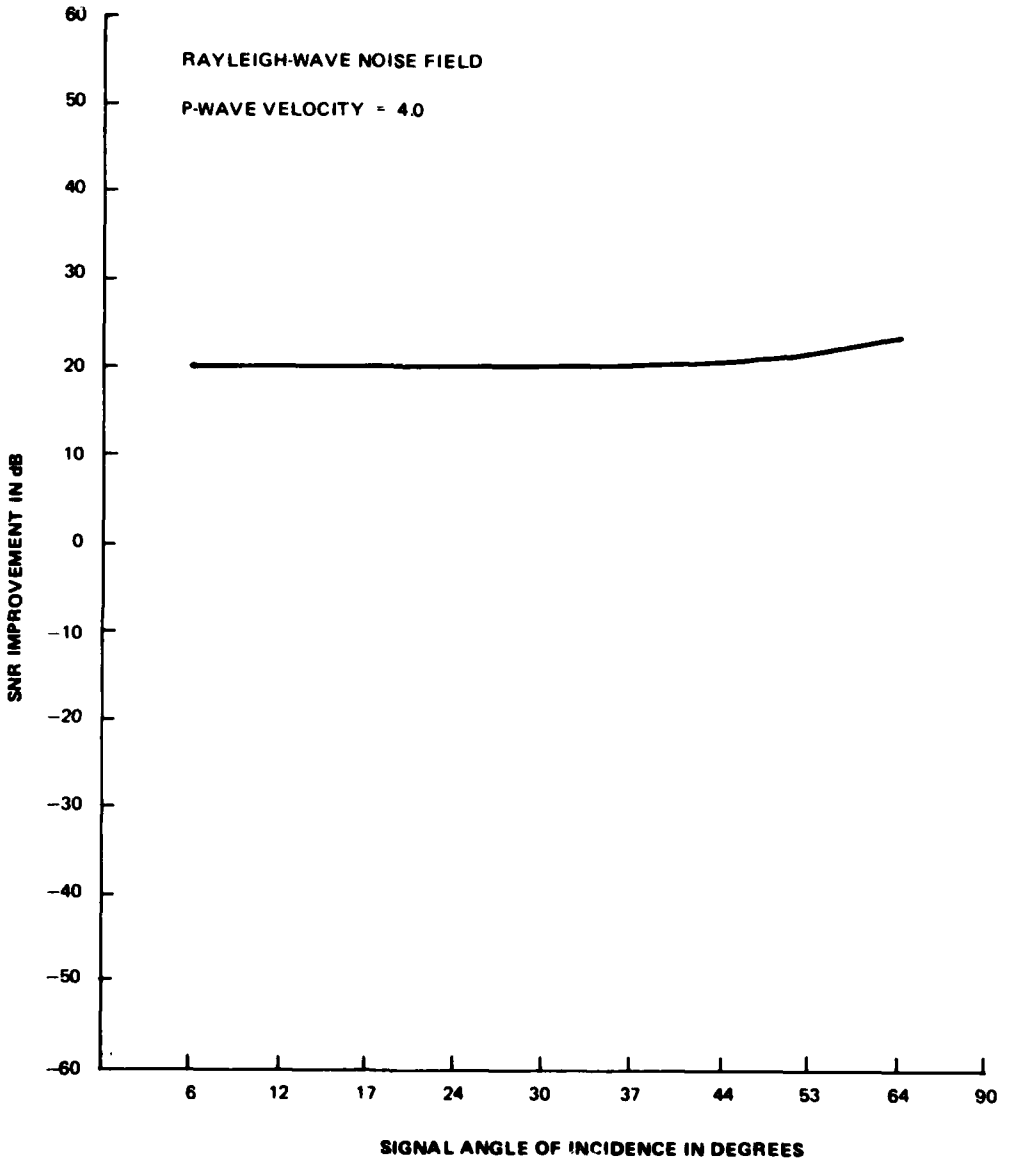

FIGURE 10. THEORETICAL P-WAVE SNR ENHANCEMENT IN A RAYLEIGH-WAVE NOISE FIELD CONTAMINATED BY 1% STRAIN SYSTEM NOISE POWER

G 11260

Therefore the SNR enhancement is controlled by the sum of the system and wind noise powers observed at the output of the strain sensor.

We also observed in section 2.4.3 that if the noise consists of scattered Rayleigh waves contaminated by "mantle P waves" then prediction error filtering will reject the Rayleigh wave noise leaving the mantle P wave component untouched. In other words the noise prediction filter predicts only the Rayleigh wave component. Thus, based upon our previous discussion, the effects of signal distortion may be neglected. Under these circumstances the SNR enhancement becomes

$$I \approx \frac{1}{B_p} \tag{67}$$

where, in this instance, B_p is the ratio of the mantle P wave noise power to the total noise power as observed at the output of the inertial sensor.

As a final example let us consider SNR enhancement in a noise field consisting of scattered P waves. Combining the results shown in figures 7 and 9 according to equation 64 yields the SNR enhancement data shown in figure 11. Comparison of these results with the signal distortion curves shown in figure 9 illustrate that for this particular type of noise field the SNR enhancement produced by prediction error filtering is significantly influenced by signal distortion. It is also worth noting that the P wave SNR enhancement can be substantial if the angle of incidence of the signal is greater than the angles of incidence characterizing the noise field.

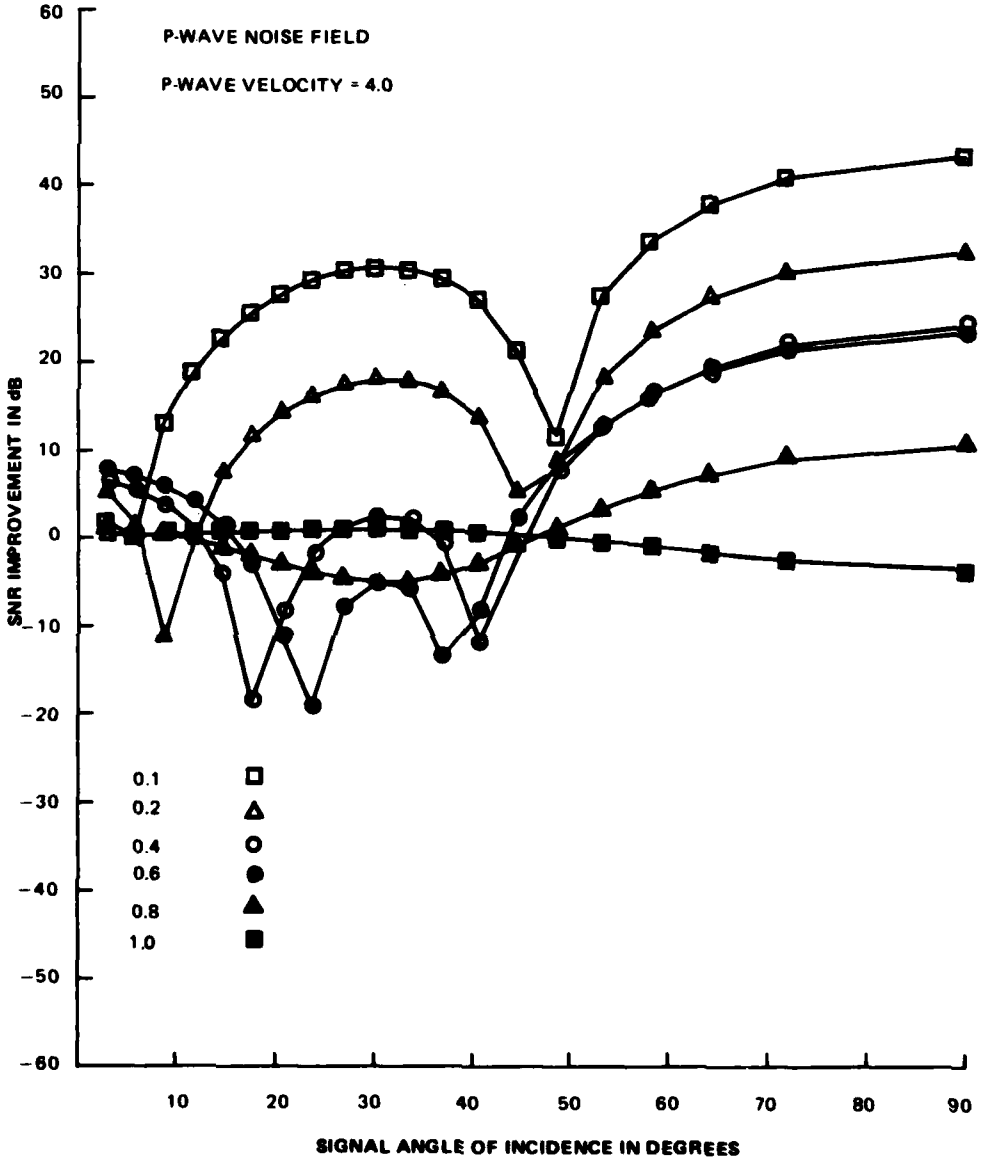

FIGURE 11. THEORETICAL P-WAVE SNR ENHANCEMENT IN A SCATTERED P-WAVE NOISE FIELD

G 11261

3. GENERAL DESIGN AND INSTALLATION CRITERIA

3.1 SYSTEM NOISE CRITERIA

The arguments developed in the previous section demonstrate that a vertically oriented S-I system has the potential for wide band isotropic P wave SNR enhancement. Furthermore, they provide theoretical confirmation of past experimental observations which have indicated that relatively high system and wind noise levels at the output of the strain sensor, as well as compositionally complex earth noise fields, have been the principal factors inhibiting the realization of this potential. More importantly, however, they provide the technical insight necessary to develop a systematic program to minimize the impact of these factors on the P wave SNR enhancement capabilities of future S-I systems. For example, as shown by equation 64, given optimum earth noise conditions (i.e. scattered Rayleigh waves of one mode) the P wave SNR enhancement capabilities of a vertically oriented S-I system will vary inversely in proportion to the ratio of the system noise power to the total noise power at the output of the strain sensor. In other words, a first prerequisite to the effective utilization of an S-I SNR enhancement system is to maintain strain system noise levels low in comparison to earth noise levels in the bandwidth of interest. This is not a trivial problem when one is interested in the enhancement of P wave SNRs in the 0.5 to 20 Hz bandwidth. A few simple calculations are sufficient to illustrate this point. It is well known that in seismically quiet locations that the vertical displacement background noise level is of the order of a few millimicrons or less at frequencies of 1.0 Hz and greater. For the purposes of demonstration let us assume that this noise consists solely of one Rayleigh mode with a phase velocity of 1 km/sec. Then utilizing equation 3.34 in section 3.2 of the Appendix it can be shown that the corresponding vertical strain noise in the vicinity of one Hz will be of the order of 10^{-12}. Now typical system noise levels for vertical strain sensors used in previous experiments were optimistically estimated to be about 2.5×10^{-12} in the vicinity of one Hz (Shopland and Kirklin, 1969). Thus according to equation 64, the maximum P wave SNR enhancement that could have been achieved under these conditions could not be more than a few dB. An important implication of this simple illustration is that because of the system noise problem we have never been able to test the S-I concepts in seismically quiet regions. While it may be argued, with some justification, that the presumably complex structure of the ambient earth noise in such regions rules out the effective utilization of an S-I system, the experimental data to support this position is almost totally lacking. Furthermore, it is worth noting that if the earth noise in such regions does consist solely of P waves with near vertical angles of incidence, as some observers have suggested, then, as shown in section 2.6, our theoretical calculations indicate that large regional P wave SNR gains may be possible. In order to experimentally test this possibility we must have a strain sensor with a system noise level of 10^{-13} or less in the 0.5 to 20 Hz bandwidth.

3.2 INSTALLATION DEPTH CRITERIA

The fabrication of a high sensitivity strain sensor is only the first step in the implementation of an effective S-I P wave SNR enhancement system. It can be seen from the arguments presented in section 2.4.2 that at a surface location wind noise and strain system noise have essentially the same impact on the P wave SNR enhancement capabilities of a vertically oriented S-I system. Unfortunately, as indicated by the following argument, the wind noise problem can be potentially far more severe than the system noise problem. It has been shown both theoretically and experimentally that the earth's response to the turbulent pressure fluctuations associated with the local wind can be a major source of seismic noise. Consider, for example, an observation point at the surface of a homogeneous and isotropic half space for which $\lambda=\mu$ and μ is of the order of 10^{10} microbars. Then from equation 5.11 in section 5.2 of the Appendix it can be seen that a pressure fluctuation of only one microbar will produce a vertical strain of about 10^{-10}. This is roughly 2 orders of magnitude greater than the vertical strains associated with the Rayleigh wave noise discussed earlier. Thus, at seismically quiet sites where the strain sensor is located at or very near the surface of the earth the strain output at frequencies greater than 1.0 Hz will be dominated by wind noise during intervals of local atmospheric turbulence. This phenomenon was observed during early S-I experiments at WMSO and while the specific nature of the problem was never recognized, the correct solution was implemented. They chose to install the vertical strain sensor at a depth of about 18 meters. Utilizing the results obtained later by Sorrells (1971) it can be shown that the attenuation of pressure generated vertical strains with depth in a half space in which $\lambda=\mu$ is given by

$$\psi \left(\frac{d}{\ell}\right) = \left(\frac{1}{2} + 2\pi \frac{d}{\ell}\right) \exp\left(-2\pi \frac{d}{\ell}\right) \tag{68}$$

where d is the depth, ℓ is the convective wave length for the pressure change and ψ is the ratio of the vertical strain at depth d to the vertical strain at the surface. Now at frequencies greater than 0.5 Hz the convective wave lengths for wind generated pressure changes will probably rarely be greater than 20 meters or so. Thus for the WMSO experiment $\frac{d}{\ell}$ would generally be less than or approximately equal to 1. Therefore

$$\psi \geq \left(\frac{1}{2} + 2\pi\right) \exp(-2\pi) \tag{69}$$

$$\geq 38 \text{ dB}$$

In other words, installation of the vertical strain sensor at a depth of 18 meters should reduce the wind noise by roughly 2 orders of magnitude or more. Therefore, the wind noise at the input to the buried sensor would probably be no more than 10^{-12} at frequencies greater 0.5 Hz. This is roughly the same order of magnitude as the strain system noise. Thus, for all practical purposes, the shallow burial technique implemented during the WMSO experiments was sufficient to eliminate the wind noise from the visual records. Earlier,

we determined that strain system noise levels on the order of 10^{-13} in the 0.5-20 Hz bandwidth were needed in order to test the S-I method in seismically quiet regions. Since wind noise imposes an identical limit on the P wave SNR enhancement capabilities of a vertically oriented S-I system we must impose the same constraint on the maximum acceptable wind noise level in the bandwidth of interest. In order to realize this constraint we must install the S-I system at depths greater than the 18 meters used in the past. Based upon calculations utilizing equation 68 the minimum "safe" depth for the installation of future systems should probably be no less than 30-40 meters.

3.3 SYSTEM DIMENSIONS

It should be recalled that in our theoretical development, colocated sensors and point strain observations were invariably assumed. The practical implications of these comments merits further comment. It is a well known experimental fact that if the earth noise field is sampled at separate points the degree of coherence between the observations trends to diminish monotonically as the separation distance increases. Thus as a general rule

$$\gamma_{ii}^2 (\delta r,\omega) < 1 \quad \delta r \neq 0 \tag{70}$$

where δr is the separation distance between the two observation points and the repeated index ii mean that identical inertial component of earth movement are sampled at the two observation points. It can also be shown that for earth noise fields which vary spatially as well as temporally.

$$\gamma_{ei}^2 (\delta r,\omega) \leq \gamma_{ii}^2 (\delta r,\omega) \quad \delta r \neq 0 \tag{71}$$

where the index, ei, denotes a strain component of earth movement is observed at one point while an inertial component is observed at the other. The equality holds for the special case where the field is a plane wave. Thus the square of the simple coherence between inertial outputs separated by a distance, δr, may be taken as the upper bound on the square of the simple coherence between strain and inertial outputs separated by the same distance. Now for the purposes of illustration, let us assume that the earth noise consists of waves whose apparent horizontal velocities are contained in the interval $\infty \leq c \leq c_\ell$ and that the power spectral densities of the individual waves are independent of their velocities. In this instance, it can be shown that the square of the simple coherence between two vertical inertial outputs is given by

$$\gamma_{ii}^2 (\delta r,\omega) = \frac{4c_\ell^2 J_1^2(\frac{\omega \delta r}{c_\ell})}{\omega^2 \delta r^2} \tag{72}$$

where $J_1(\xi)$ is a Bessel function of the first kind and order 1. Now it has been shown in section 2.4 that neglecting the effects of signal distortion the SNR enhancement capabilities of a vertically oriented S-I system is given by

$$I = \frac{1}{1 - \gamma_{ei}^2}$$

Therefore for the problem under consideration

$$I \leq \frac{1}{1 - \frac{4\, c_\ell^2\, J_1^2 \left(\frac{\omega \delta r}{c_\ell}\right)}{\omega^2\, \delta r^2}} \tag{73}$$

Now suppose we require that the limitations on P wave SNR enhancement arising from lateral separation of the strain and inertial sensors be no greater than the strain system noise and wind noise constraints; i.e.

$$I_{min} \geq 100 \tag{74}$$

Applying this condition yields

$$\delta r \leq 0.06 \frac{c_\ell}{f} \tag{75}$$

where f is the frequency in Hz. Now there are regions where c_ℓ may be of the order of a few hundred meters per sec or less whereas we are interested in P wave SNR enhancement at frequencies as high as 20 Hz. Thus in order to avoid significant limitations on the SNR enhancement capability of an S-I system at high frequencies which arise from noise field decorrelation, the separation distance between the strain and inertial sensors should be no more than a few meters at the most. Hence, strict adherence to the colocation assumption is critical to the successful utilization of an S-I system for regional P wave SNR enhancement.

By a similar line of reasoning it can be shown that similar constraints apply to the separation distance between the sensing elements of the strainmeter; i.e. if one wishes to effectively utilize the S-I method of P wave SNR enhancement at frequencies as high as 20 Hz in noise fields where the horizontal velocities may be as low as a few hundred meters/sec then the strain and length should be no more than a few meters at the most. In other words the strain measurement should closely approximate a point observation.

3.4 INSTALLATION NOISE

At this point in our discussion we should logically consider the magnitude and the means for controlling "installation noise". By this term we mean that which might arise from sources immediately adjacent to the S-I system. Unfortunately, we have neither the experimental data nor the theory to attack this problem at this time or even to determine whether it will substantially limit the P wave SNR enhancement capabilities of an S-I system. Let us state therefore that our goal is to maintain strain installation noise at or below the 10^{-13} level in the bandwidth 0.5 to 20 Hz. If preliminary experiments with prototype models of future S-I systems demonstrate that this goal is not

achievable then investigations must be carried out to develop methods for minimizing the impact of this type of noise on the P wave SNR enhancement capabilities of an S-I system.

3.5 SUMMARY OF DESIGN AND INSTALLATION CRITERIA

The principal design and installation constraints developed in the previous sections may be briefly summarized as follows.

1. Strain System Noise Level: 10^{-13} in the 0.5-20 Hz bandwidth.
2. Maximum Linear Dimensions: Less than 3 meters.
3. Minimum Installation Depth: 40 meters.
4. "Installation" Noise Level: 10^{-13} in the 0.5 - 20 Hz bandwidths.

4. CONCEPTUAL DESIGN FOR AN ADVANCED STRAIN-INERTIAL SEISMOGRAPH SYSTEM

4.1 GENERAL DESCRIPTION

A conceptual design for a vertically oriented S-I system, capable of installation in a shallow-borehole, and which generally satisfies the design constraints discussed in the previous section, has been developed. The unit, which has been designated, the Strain-Inertial Seismograph System, Model 52000, will contain components to sense vertical displacement and differential vertical displacement (vertical strain) to filter, and combine the strain and inertial outputs and to display both the individual and combined outputs as a function of time.

As shown by the block diagram in figure 12, 4 major interfaces conceptually divide the system into 3 major components, the borehole, the S-I seismometer and the wellhead terminal. These components are discussed in greater detail in the following paragraphs.

4.2 S-I BOREHOLE

The S-I borehole will be engineered to satisfy certain special conditions. In particular, as shown in figure 13, one section of the borehole casing will contain a precision instrument support. This support will be welded to a casing section then stress relieved prior to entry into the borehole. It will then be joined to standard casing to place the support at a preselected depth.

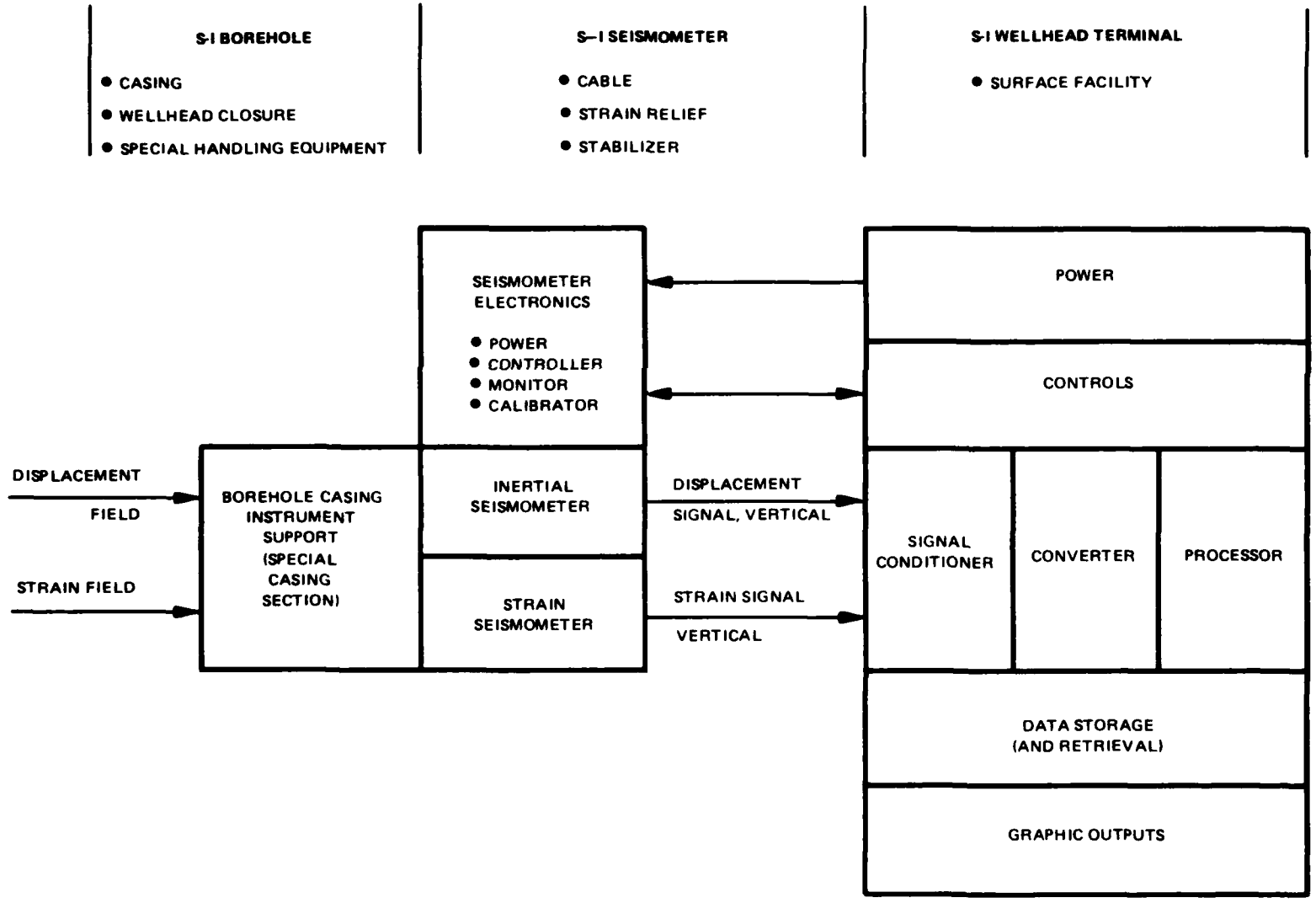

FIGURE 12. STRAIN-INERTIAL SEISMOGRAPH SYSTEM BLOCK DIAGRAM

G 11262

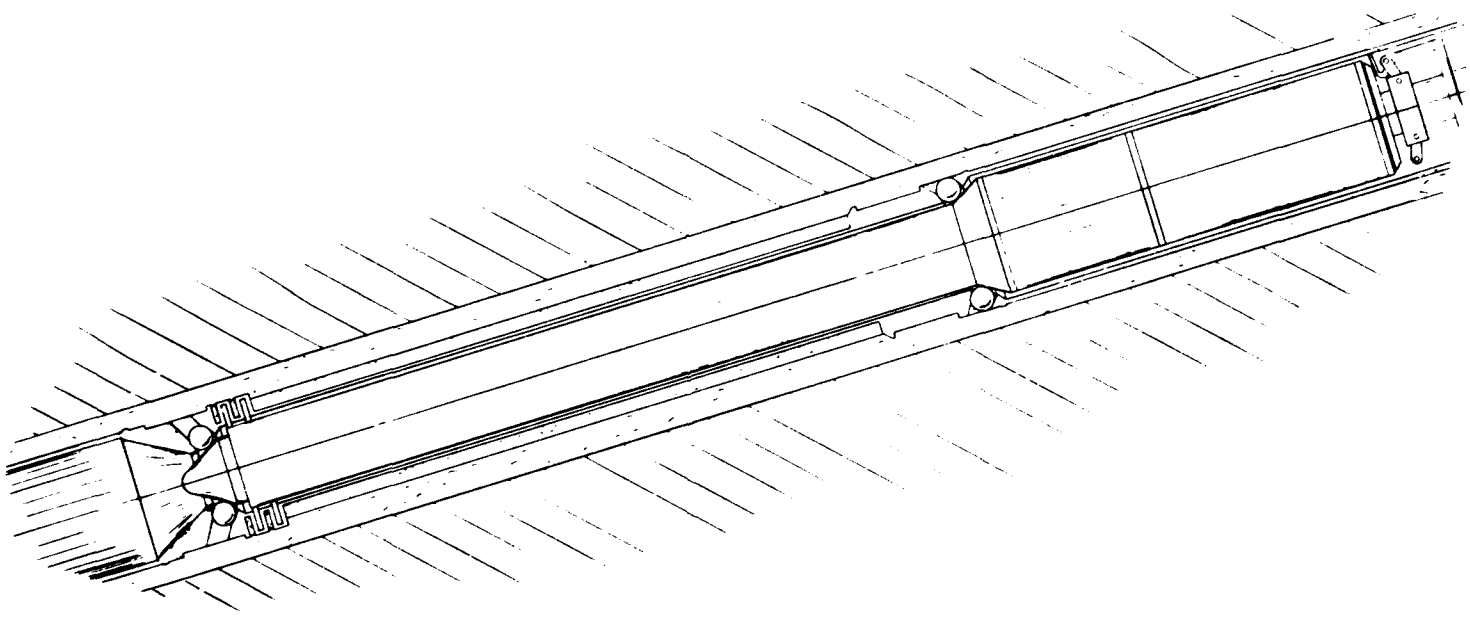

FIGURE 13a. STRAIN INERTIAL SEISMOMETER INSTALLATION SPECIAL CASING SECTION

G 11263

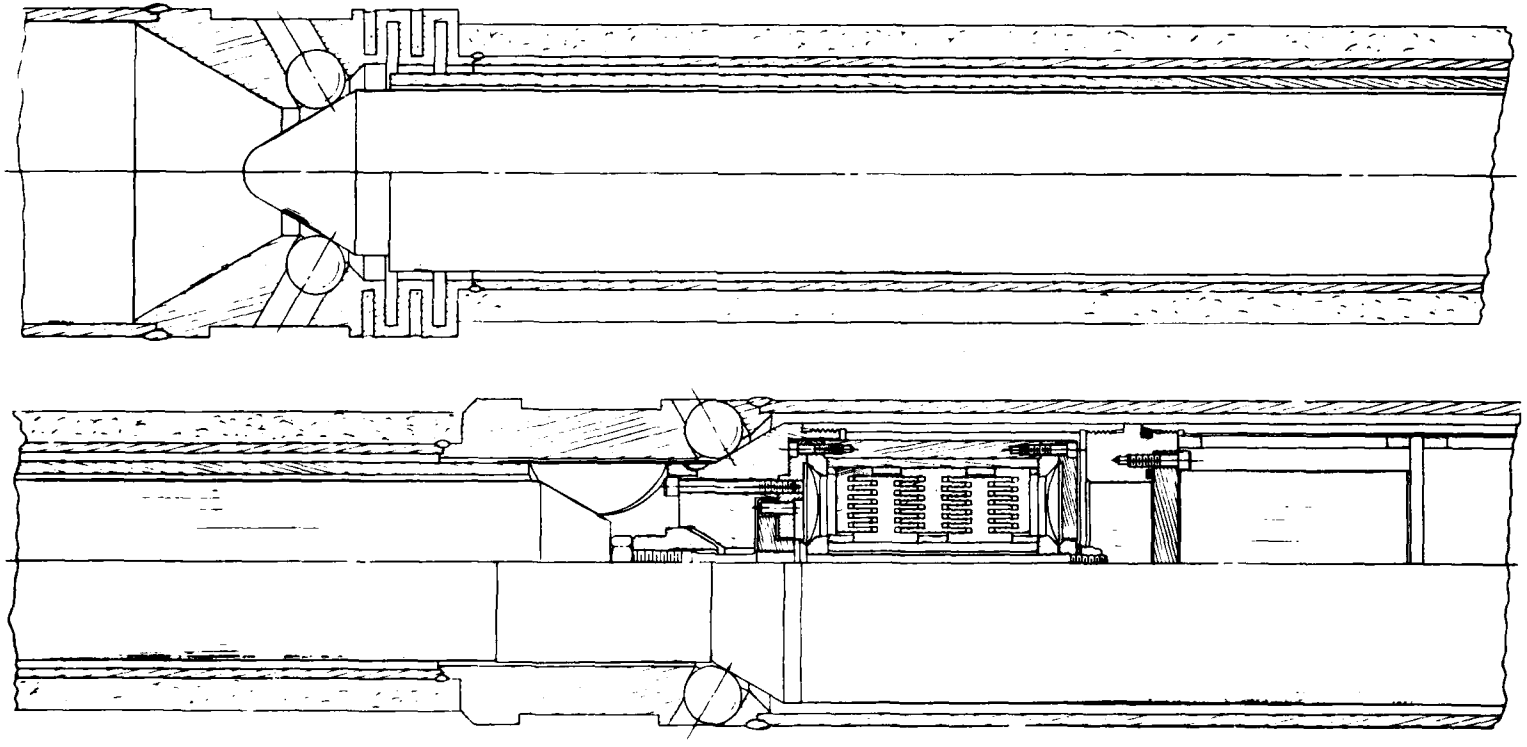

FIGURE 13b. CROSS SECTIONAL VIEW OF STRAIN ROD AND STRAIN TRANSDUCER

G 11264

Since the support prohibits float shoe/squeegee cementing treatment, the cement will be applied externally to the casing. The cement will be chosen to optimize the interface between the casing and the local formation.

The minimum borehole depth and maximum deviation angle will be appropriate for high frequency P wave enhancement (i.e., frequencies greater than 1.0 Hz).

4.3 THE S-I SEISMOMETER

The S-I seismometer consists of an element which senses linear differential displacement between the upper and lower instrument supports (the strain seismometer) and an element which senses acceleration at the upper seat of the instrument support (the inertial seismometer). It also contains electronics for power conditioning, communication control and monitoring.

The strain seismometer consists of the strain rod assembly, the strain transducer assembly and the associated electronic circuitry.

The strain rod will be matched to the borehole casing support and will operate under essentially constant stress conditions. The strain transducer will achieve a large linear travel range ($\pm$2 mm typical) by using a variable-coupling type capacitor construction. Desired resolution will be achieved by operating 4 independent capacitance bridges with summation after amplification. Consideration will also be given to organizing the bridges in quadrants to provide the capability to sense horizontal differential displacements.

The strain seismometer electronic circuitry will perform the following functions:

a. Capacitance bridge excitation;

b. Capacitance bridge output amplification;

c. Bridge signal summation, amplification, and demodulation;

d. Develop low-gain dc-coupled output;

e. Develop high-gain short period output.

The high-gain, short period output will be the primary signal output. Its characteristics will not be altered by the presence of large (10^{-7} m/m) long term strain components. Depending on whether "quadrant" or "linear-only" organization of the transducer assembly is utilized, electronic circuits will be provided for each primary output. Overall, the design of the strain seismometer is expected to minimize the effects of temperature gradients, pressure gradients residual stresses, spurious modes and cross axis disturbances.

The conceptual design includes a vertical KS-36000 as the inertial sensor. It will be used without leveling mechanism to maintain alignment with the strain sensor. It can accommodate tilts of 3-4 degrees at temperate latitudes

and temperatures. Special adjustments will have to be made to accommodate extreme conditions. The inertial electronic circuits will be similar or common with those of the strain seismometer.

It is possible that two other inertial seismometers, the S-700 and the 44000, could replace the KS-36000 in the S-I system. In general, for these units to qualify for use in the S-I system, the response should not change over the short period band (0.5-10 Hz) and the short period seismometer noise should not exceed 3×10^{-7} $(m/sec^2)^2/Hz$. While the 20171A (or 23900) satisfies the noise constraint, its response and response stability characteristics make it less desirable for the S-I system.

4.4 THE WELLHEAD TERMINAL

The S-1 wellhead terminal will perform the following functions

a. Power conditioning

b. Operating controls

c. Signal conditioning

d. Data conversion

e. Data storage and retrieval

f. Data processing

g. Data display

Power conditioning will be provided by the wellhead terminal power assembly which interfaces with the primary power source at the site. It will provide power to the terminal and the S-I seismometer. A signal conditioner will interface with the S-I seismometer signal outputs and will provide analog response and shaping and anti-alias filtering for primary data channels. The conditioned signals will be applied to a data converter and may be selected for display.

Initially, the individual strain and inertial conditioned signals will be digitized and recorded on magnetic tape at the site. The strain and inertial data will then be examined in conjunction with supplementary noise field data to determine optimum P wave enhancement processing techniques. After processing definition specifications will be prepared for the S-I converter and processor.

4.5 SUMMARY OF PRIMARY SYSTEM CHARACTERISTICS

The primary characteristics for the major components of the S-I system are summarized below:

Borehole

Depth	40 meters, (131 ft)
Casing diameter	7 inch o.d., 20 lb/ft, API
Slant angle	3-degrees

Strain-inertial seismometer

Noise power, eq, input	
Strain	4×10^{-26} $(m/m)^2/Hz$
Inertial	1×10^{-18} $(m/s^2)^2/Hz$
Primary output response	
Strain	1×10^{8} volt/(m/m), 0.2 to 10 Hz
Inertial	3×10^{4} volt/(m/s), 0.2 to 10 Hz
Secondary output	
Strain	5×10^{5} volt/(m/m), dc to 10 Hz
Inertial	1×10^{3} volt/(m/s^2), dc to 10 Hz
Strain rod length	1 meter

Wellhead terminal

Characteristics of the wellhead terminal assemblies will evolve with the acquisition and operating systems. Initially, the SDCS acquisition equipment can be used with special signal conditioning circuits.

5. GENERAL UTILIZATION CONSTRAINTS

Development of the S-I seismograph system, whose conceptual design was discussed in the previous section, will eliminate many of the problems that plagued earlier attempts to reduce the S-I method of P wave SNR enhancement to practice. The remaining questions surrounding its ultimate value to the underground nuclear test detection program relate to the nature of the propagating earth noise field in the 0.5-20 Hz. In this regard, certain general constraints upon the effective utilization of an S-I system are worth noting. The S-I method was originally conceived to enhance P wave SNRs in the presence of earth noise consisting of scattered Rayleigh waves of a single mode. As we have seen from the discussion in section 2, it will perform remarkably well under these conditions, being limited only by the fractional power of the system and wind noise power at the output of the strain sensor in the bandwidth of interest. As the earth noise field departs from this simple structure the SNR enhancement capabilities of the S-I system will diminish. The simple example of a field consisting of Rayleigh waves and "mantle" P waves succinctly illustrates this point. We see from the results of section 2 that in this instance the S-I system will simply strip away the Rayleigh waves leaving the mantle P wave noise intact. More generally we may infer from this example, that if the noise field contains well organized high and low velocity components in the bandwidth of interest then the fractional power characterizing the high velocity component establishes the limit on the P wave SNR capabilities of the S-I system. In other words if the noise power is dominated by a high velocity component then the P wave SNR enhancement capabilities of an S-I system will be negligible. The term 'is dominated' requires some further clarification. We have seen in section 2 that if the earth noise consists entirely of P waves with near vertical angles of incidence, large P wave SNR gains for regional signals are theoretically possible. Thus there exists a narrow power range in which the SNR enhancement capabilities may actually increase as the percentage of high velocity earth noise increases. From the results contained in section 2 this range is approximately defined by

$$0.999 \leq B_p \leq 1 \tag{76}$$

where B_p is the ratio of the high velocity noise power to the total noise power observed at the output of the inertial sensor. Therefore, the SNR enhancement capabilities of an S-I system will generally be degraded by the addition of a high velocity noise component to a Rayleigh wave field provided that B_p lies in the interval.

$$0 \leq B_p < 0.999 \tag{77}$$

Outside this interval large regional P wave gains may be possible. This latter condition will hold, however, only if the noise consists of P waves with near vertical angles of incidence. If the P wave noise field contains components with angles of incidence as large as 12°-15°, the use of an S-I system can reduce rather than enhance regional P wave SNRs. Thus, effective utilization of an S-I system in a high velocity noise field requires a special set of conditions which may be difficult to realize in practice.

Overall, then, we see that even though development of an advanced S-I system will largely eliminate the design and installation problems encountered during previous experiments, its P wave SNR enhancement capabilities will still be constrained by the composition and state of organization of the earth noise in the bandwidth of interest. The general nature of the earth noise in the regional signal bandwidth is briefly discussed in the following section.

6. EARTH NOISE IN THE REGIONAL SIGNAL BANDWIDTH

6.1 REVIEW OF EXISTING DATA

For our purposes, the regional signal bandwidth is considered to cover the frequency range $0.5 < f < 20$ Hz. During the past two decades the noise in this bandwidth has been the subject of numerous investigations. In particular, the need to develop reliable methods for the enhancement of teleseismic signals led to the deployment of large scale horizontal arrays and deep borehole seismograph systems during the mid-1960s. The data provided by these sensor systems formed the basis of several experimental studies in the late 1960s and early 1970s which yielded a fairly comprehensive qualitative picture of the earth noise at frequencies less than 2 or 3 Hz. For our purposes it is worth noting that in the interval 0.5-1.0 studies of the data from the Montana LASA (Toksoz and Lacoss, 1968, Haubrich and McKamy, 1969, Lacoss et al, 1969, Capon 1969) indicate that the earth noise in this band is predominantly body waves mixed with higher mode Rayleigh waves. Analysis of the data from deep borehole seismograph systems is also consistent with this description (Douze, 1967). This noise appears to be derived principally from oceanic sources, although there is some evidence that local or regional sources may make significant contributions during quiet intervals (Iyer and Healy, 1972, Capon 1973). The relative power levels of the individual components tends to vary as a function of frequency and as a function of time. In particular, high body wave noise levels appear to be correlated with storms at sea (Haubrich and McKamy, 1969).

As shown in figure 14 there is a distinct change in the slope of the ambient earth noise spectrum near 1.0 Hz. This slope change is thought to mark the transition from "oceanic" to locally generated noise. Much less is known about the composition and structure of this local noise. However, synthesis of the results from investigations related to underground nuclear test detection (Frantii et al, 1962, Douze 1964, 1967, Robertson, 1965, Sanford et al 1963, Fix 1972) and from experimental assessments of the "ground noise" geothermal exploration method (Clacy, 1968, Whiteford, 1970, 1975; Douze and Sorrells, 1974; Goforth et al, 1972, Iyer and Hitchcock 1974, 1976; Liaw and McEvilly, 1979) yields a hypothesis concerning the major components of the earth noise at frequencies greater than one Hz. The hypothetical power spectral densities of these components are schematically illustrated in figure 13 and are discussed in greater detail in the following paragraphs.

Curve 1 represents the power spectral density of a residual component commonly observed at sites that are isolated from both cultural and naturally occurring sources. Typical features include one or more peaks in the 2-4 Hz range

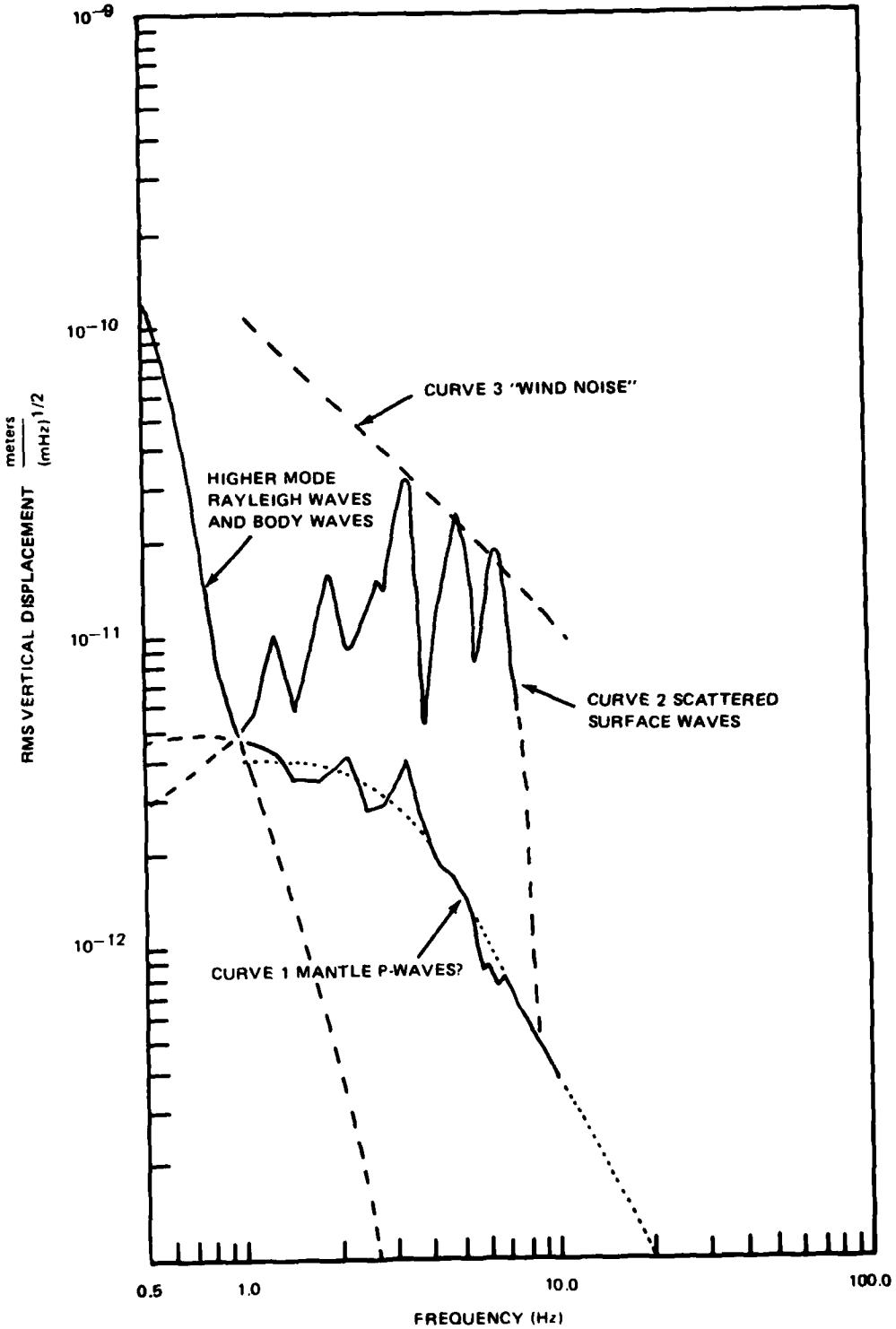

FIGURE 14. SPECULATIVE MODEL OF THE EARTH NOISE SPECTRUM IN THE REGIONAL SIGNAL BANDWIDTH

G10732A

followed by a more or less featureless band in which the spectral amplitude diminishes as the inverse square of the frequency. This particular estimate was computed from data collected at Queen Creek, Arizona (Fix, 1972). Very similar spectral envelopes characterize the noise observed at Kanab, Utah (Frantii et al, 1962) and at the Ogdensburg mine during quiet intervals (Isacks and Oliver, 1962). It has been suggested that the residual component consists primarily of body waves arriving at near vertical angles of incidence (so called mantle P waves). However, this explanation is based largely on limited observations at frequencies at less than 2-3 Hz. Thus, in our opinion, the composition of this component is largely undefined at this time.

At sites where nearby cultural or naturally occurring sources are intermittently active the residual component is commonly overridden by a second component whose spectral density is schematically illustrated by curve 2 in figure 14. This component will be referred to as the surface wave component because it is believed to consist primarily of fundamental mode Rayleigh waves. However, there is evidence to suggest that the individual peaks in its power spectral density may be associated with the local group velocity minima of higher mode Rayleigh waves (Asten, 1978). The shape of the spectral envelope seems to be strongly dependent on the local velocity structure in the uppermost few hundred meters of the earths crust and in some instances may be largely determined by the structure in the uppermost few 10s of meters (Liaw and McEvilly, 1979). The time dependence and intensity of the noise sources may also play a significant role in determining the local spectral envelope of this second component. However, source effects have been clearly documented in only a few isolated instances (cf. Sanford, et al, 1968).

A third, wind related, component is often observed at surface sites when local wind speeds are in excess of a few miles per hour or so. The power spectral density is schematically illustrated by curve 3 in figure 14. The results of experimental studies by Douze (1964) coupled with studies by Sorrells (1971) strongly suggests that this component consists principally of near field, quasi-static deformations of the surface of the earth in response to wind generated atmospheric pressure fluctuations. The power in this component is functionally dependent upon the local atmospheric pressure power spectral density and upon the local medium response to pressure changes acting at the surface of the earth.

6.2 IMPLICATIONS

The existing data base concerning earth noise in the regional signal bandwidth is deficient for our purposes in that it fails to provide quantitative information concerning relative composition and state of organization. As we have seen from our previous discussions, the P wave SNR enhancement capabilities of any future S-I system will be critically dependent upon these factors. Thus, a complete assessment of the feasibility of developing an advanced S-I cannot be made at ths time. Nevertheless, certain generalizations are possible. For example, based upon the available data it seems very likely that an S-I system can be used to enhance P wave SNRs in regions where the surface wave component is predominant. Significant SNR gains are likely to occur only at frequencies greater than one Hz and may vary substantially within the 1-20 Hz passband depending upon the relative composition of the

noise power at different frequencies. The relative composition of the noise may also vary substantially in time as well as over relatively short lateral distances depending upon the local near surface geology. Thus the P wave SNR enhancement capabilities of an S-I system is very likely to be strongly site and time dependent in regions where the surface wave component is predominant in the regional signal bandwidth. At locations where the residual component predominates, the P wave SNR enhancement that could be obtained through the use of an S-I system must be termed highly speculative at this time. While our calculations indicate that large regional P wave SNR gains are possible, if the residual noise does indeed consist of "mantle" P waves, conclusion evidence to support this description is not currently available.

Overall, the results of the review of the existing data base demonstrate that the P wave SNR enhancement capabilities may vary from excellent to poor depending upon the nature of the local earth noise field. Thus intelligent use of future S-I systems will require a priori information about the local properties of the earth noise field in the regions where they are to be deployed.

6.3 PRELIMINARY EXPERIMENTAL RESULTS

From the foregoing discussion it should be clear that quantitative information concerning the composition and state of organization of the earth noise is necessary in order to realistically assess the P wave SNR enhancement capabilities of an S-I system. It is equally clear that the existing data base fails to provide the required levels of detail. Therefore, as a part of this project, preliminary investigations were undertaken to expand the data base pertaining to the earth noise in the regional signal bandwidth. During the course of these investigations we have adapted Liaws (Liaw, 1978) method for the estimation of high resolution frequency wave number (f-k) spectra to run on the Vax 11/780 system and have developed a working version of Abo Zena's (Abo Zena, 1979) method for calculating the phase and group velocities characterising a horizontally layered elastic solid. Abo Zena's method is particularly useful to us in that it provides us with the capability to accurately calculate the phase and group velocities for high frequency Rayleigh wave modes in thinly bedded media. In addition, preliminary field measurements were made at McKinney, Texas, in order to develop criteria for the design of future experiments at this site. The data collection system used to obtain the preliminary information was furnished by the SDCS program sponsored by AFTAC/VSC. A block diagram of the system is shown in figure 15. Basically the system consisted of six short period seismometers and signal conditioning electronics to yield samples of the earth noise in the 0.5-20 Hz bandwidth. The overall system response to a constant displacement input is shown in figure 16. In addition, a trigger mechanism was provided so that data were collected by the system only when the local wind speeds were less than 5 mph. When this condition was met, data from the 6 seismographs were sampled at 125 ms intervals and stored on magnetic tape for future analysis. The sensors were deployed in a linear array. During the measurements program the interval between sensors was changed to produce arrays which varied from 50 to 250 meters in length. The sensors were buried at a shallow-depth and care was taken to ensure that the local geology was uniform at each site in the array. An example of some of the preliminary results are shown in figure 17. These are records from the 250 meter array during an interval when the

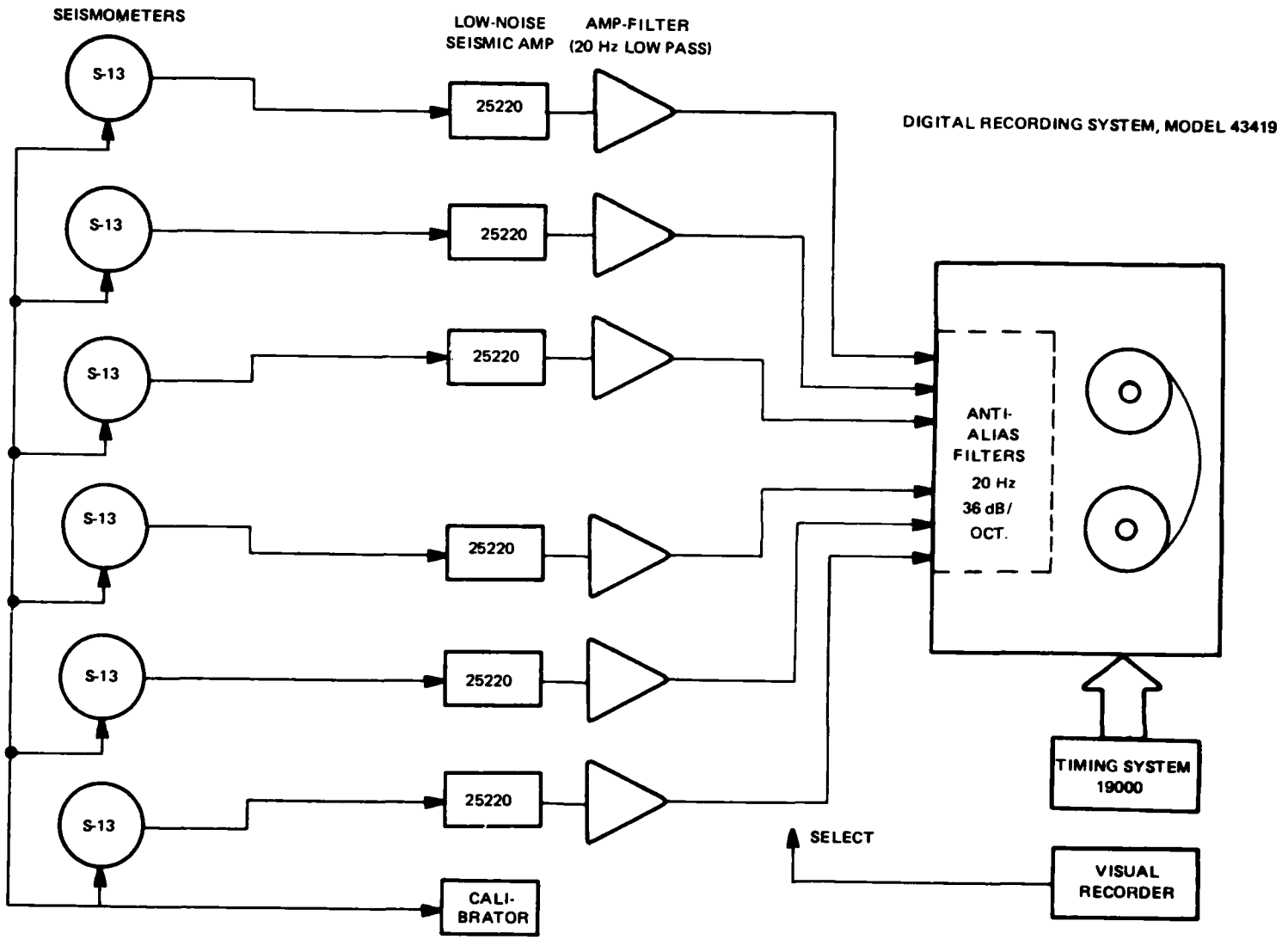

FIGURE 15. BLOCK DIAGRAM OF THE SEISMOGRAPH SYSTEM

G 11265

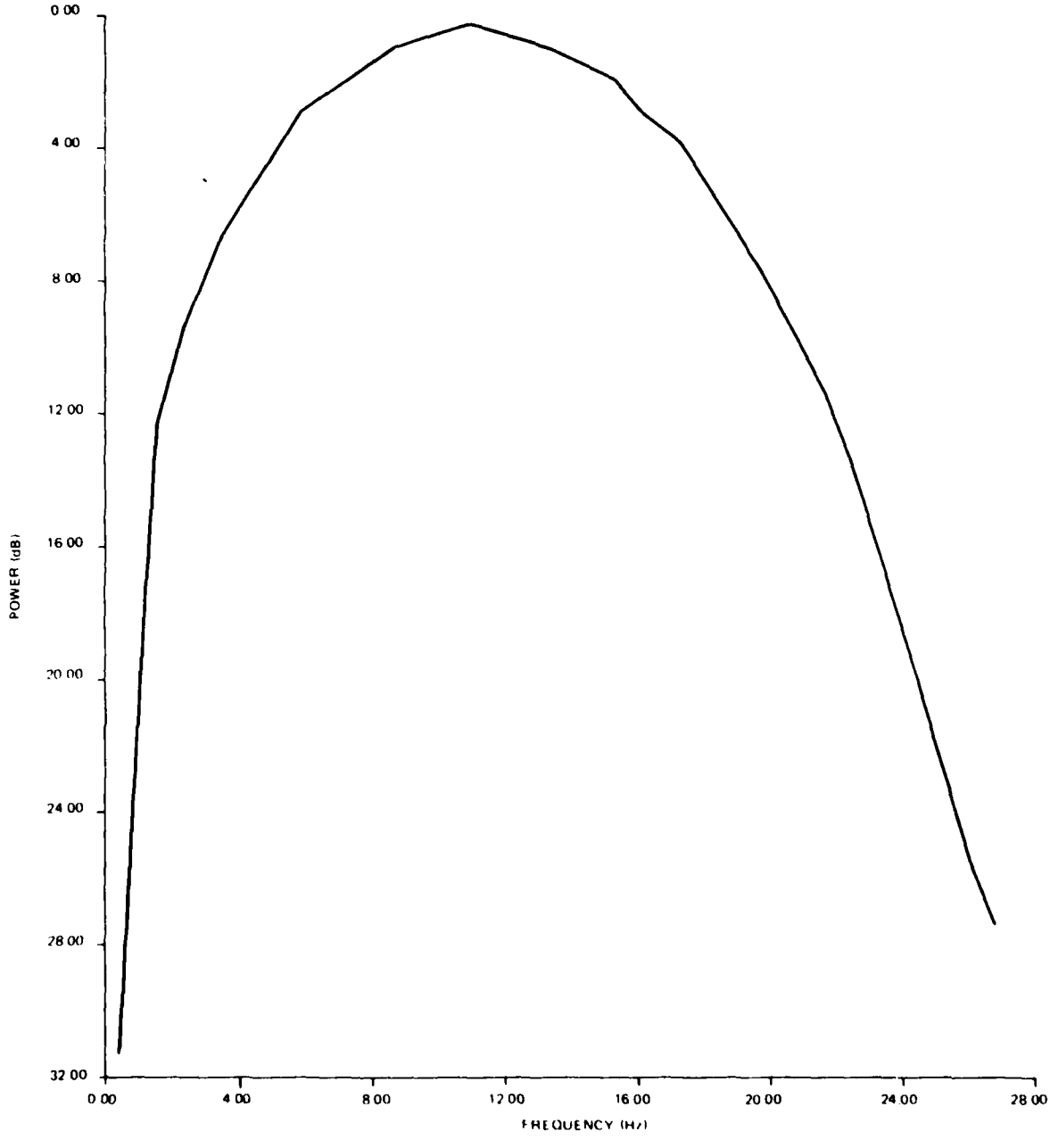

FIGURE 16. FREQUENCY RESPONSE OF NOISE DATA COLLECTION SYSTEM TO A CONSTANT DISPLACEMENT INPUT

G 11266

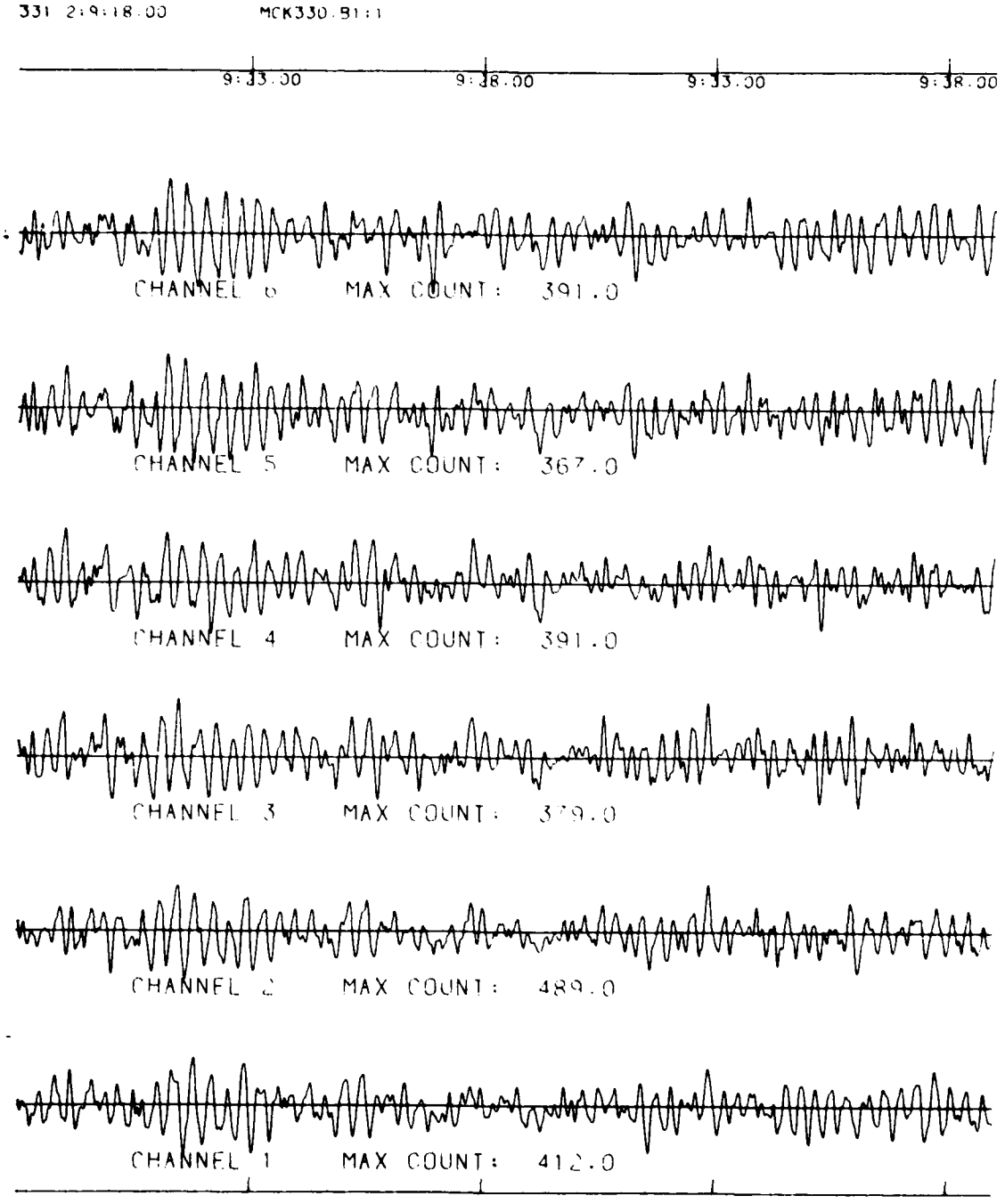

FIGURE 17. REPRESENTATIVE NOISE RECORDS AT McKINNEY, TEXAS, DURING A QUIET INTERVAL. INTERVAL BETWEEN SEISMOMETERS IS 50 METERS.

G 11267

wind speed was less than 5 mph. In addition the sample was taken when the effects of local cultural activity should be at a minimum. Observe that the records are dominated by a quasi-sinusoidal component with frequencies in the 2-4 Hz range. This component appears to be fairly well organized over the dimensions of the array. Response corrected spectral estimates for the data recorded at stations 1 and 6 (the end points of the array) are compared for reference to the Queen Creek spectral estimate in figure 18-a. The estimated square of the simple coherence between the data recorded at stations 1 and 6 is shown in figure 18-b. Notice the coherence minimum which occurs near 1.5 Hz. We suspect that this marks the transition from the body waves characterizing the oceanic component to the local noise which we believe in this case to be dominated by surface waves. As implied by the time series, the noise field power is dominated by a well organized 2-4 Hz component. In addition there is some indication of weak, organized components in the 5-8 Hz band and near 10 Hz. The difference between the McKinney and Queen Creek spectra demonstrates that even under optimum environmental conditions, McKinney is a relatively noisy site. In addition, we believe that future studies will reveal that a significant fraction of this difference is caused by the presence of low velocity fundamental and higher mode Rayleigh waves. If this is true, then McKinney would qualify as a potential site for testing the P wave SNR enhancement capabilities of future S-I systems.

Further studies of the noise at McKinney should be directed towards testing the hypothesis that a significant fraction of the earth noise in the regional signal bandwidth consists of scattered fundamental and higher mode Rayleigh waves. This will require the deployment of two dimensional spatial arrays of sensors and the computation of $(f-\bar{k})$ power spectral density estimates. In order to assist in the design of the data collection array we have made estimates of the variation of coherence as a function of separation distance. Some preliminary results are shown in figure 19. Notice that the square of the estimated coherence diminishes more or less monotonically both as a function of increasing frequency and separation distance. For all practical purposes the field at frequencies greater than about 2 Hz is seen to be completely disorganized at separation intervals on the order of a few hundred meters or so. This suggests that arrays with relatively small lateral dimensions can be used to collect the data necessary for reliable $(f-\bar{k})$ spectral estimates of the high frequency noise in the regional signal bandwidth.

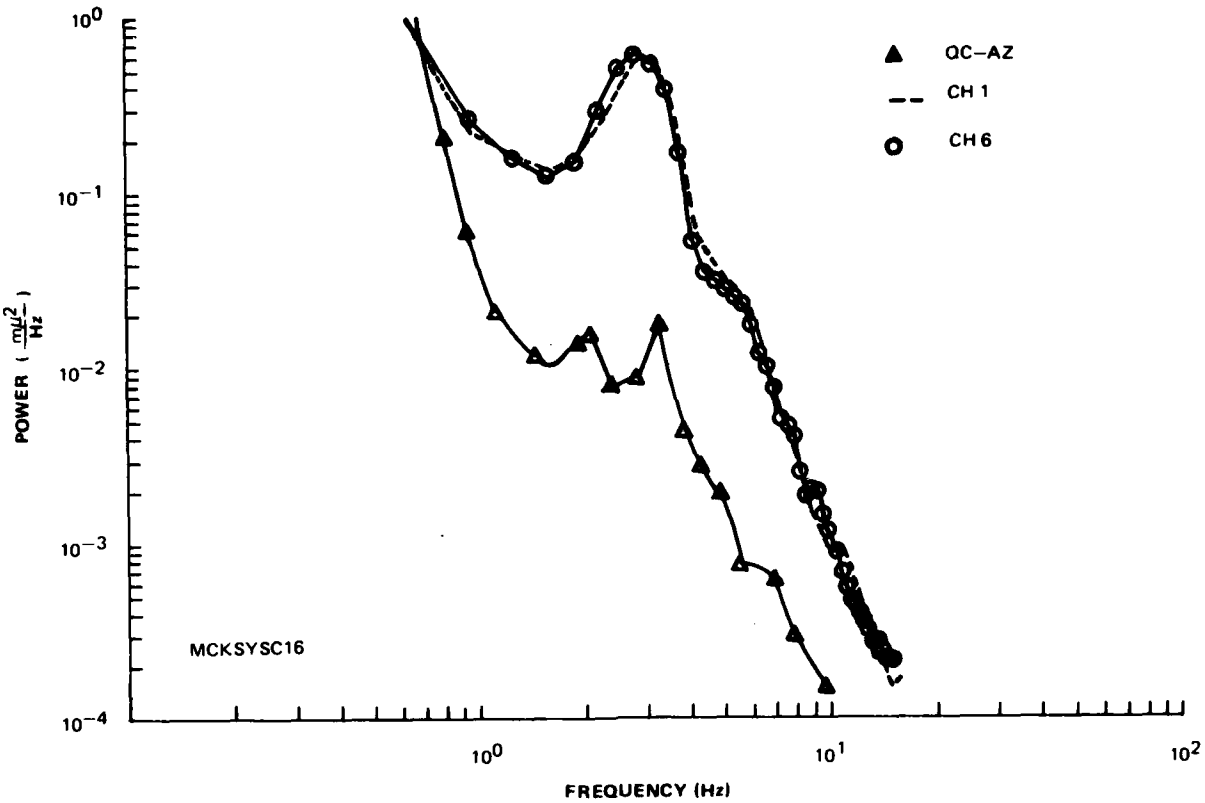

FIGURE 18. (a) REPRESENTATIVE NOISE POWER SPECTRAL DENSITY ESTIMATES AT McKINNEY, TEXAS, DURING A QUIET INTERVAL. QUEEN CREEK NOISE ESTIMATE , FIX, 1972 IS INCLUDED FOR REFERENCE.

G 11268

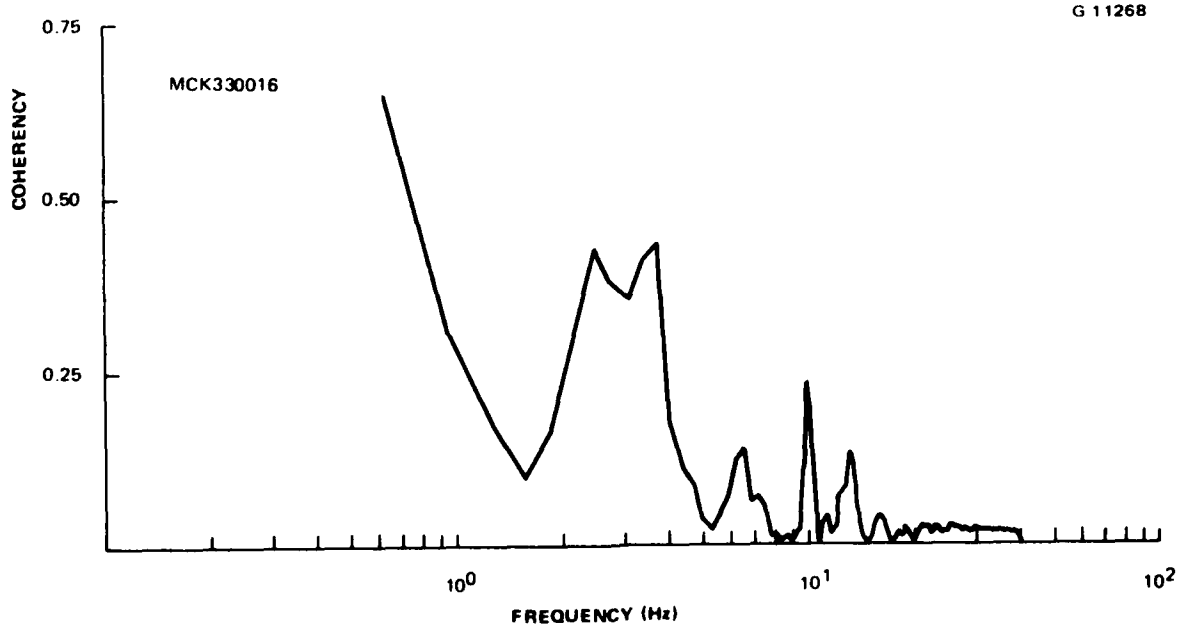

FIGURE 18. (b) REPRESENTATIVE COHERENCE ESTIMATES FOR STATIONS 250 METERS APART

G 11269

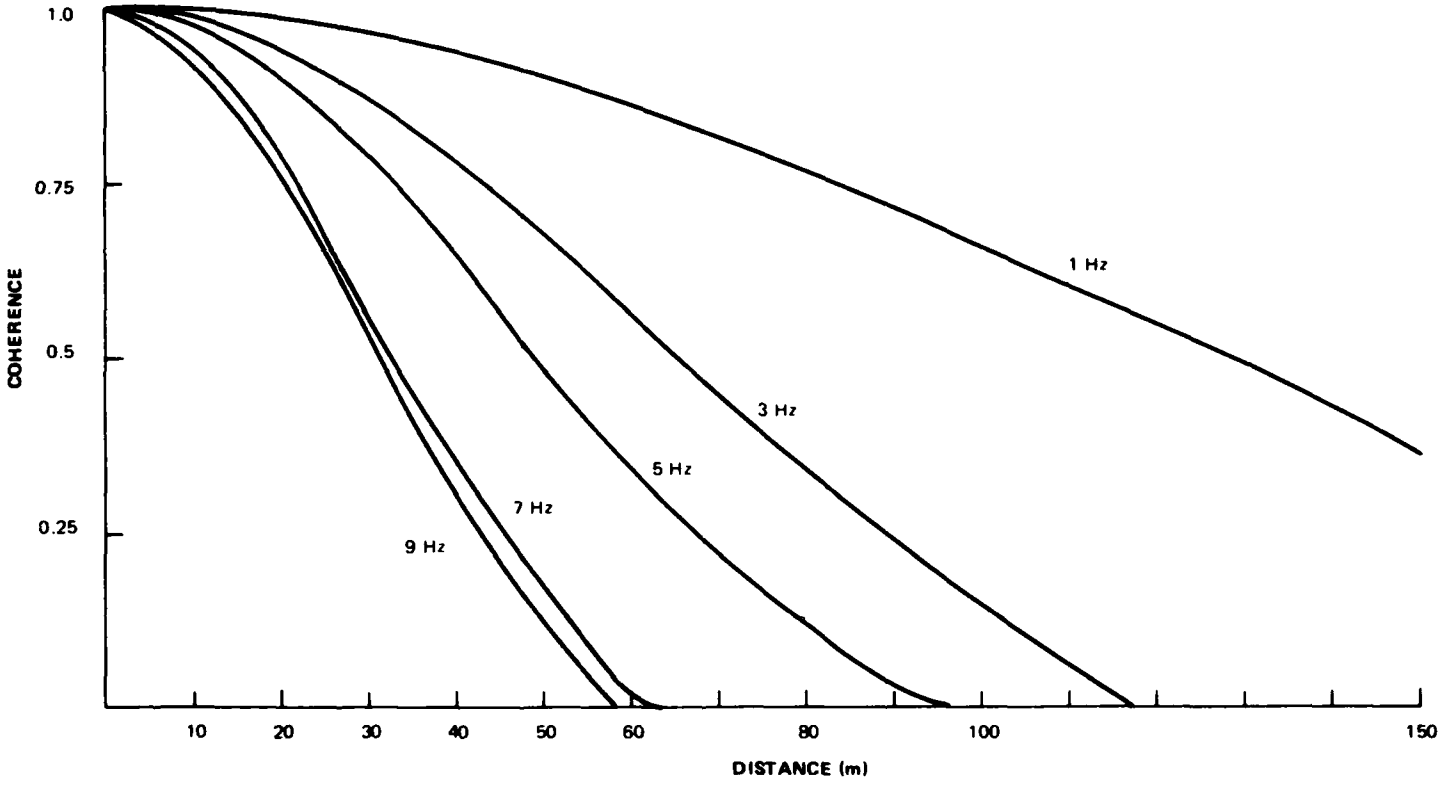

FIGURE 19. DEGRADATION OF ESTIMATED COHERENCE AS A FUNCTION OF SENSOR SEPARATION DISTANCE FOR DIFFERENT FREQUENCIES

G 11270

7. CONCLUSIONS

The results of our investigation generally demonstrate that a vertically oriented S-I seismograph system has the potential for wide band, isotropic P wave SNR enhancement. Failure to realize this potential may be attributed largely to deficiencies in system design and installation procedures which placed severe limitations on the performance of previously developed systems. These limitations can be avoided by developing an advanced S-I system which incorporates the principal elements of the conceptual design described in this document. However, minimization of the design and installation constraints will not guarantee satisfactory performance from an S-I system for its P wave SNR enhancement capability is critically dependent on the composition and state of organization of the earth noise in the bandwidth of interest. Thus, a complete assessment of S-I system P wave SNR enhancement capabilities requires quantitative information regarding these parameters. Data to the required level of detail are not generally available, particularly in the regional signal bandwidth. Nevertheless, it is worthwhile to speculate upon the regional P wave SNR enhancement capabilities of an S-I seismograph system based upon the information available to us at this time. In particular, P wave SNR enhancement is unlikely to be impressive in the "oceanic" noise band (~0.5-1.0 Hz) except perhaps at sites located near coastlines, because of the apparently high percentage of P wave noise power. As our calculations have indicated, the optimum S-I prediction error processor will simply strip away the surface wave noise leaving the P wave noise as a residual. In the "local" noise band (~1-20 Hz) P wave SNR enhancement is likely to be highly site specific and can be expected to vary substantially both as a function of time and frequency. At sites which are remote from both cultural and naturally occurring noise sources P wave SNR enhancement is generally expected to be negligible. However, the possibility that the noise at these sites consist of P waves at near vertical angles of incidence (mantle P waves) is worth checking out, for under these conditions large P wave SNRs are theoretically possible. On the other hand, regional P wave SNR enhancement may well be substantial at sites where nearby noise sources are active and the local geology will permit the existence of high frequency Rayleigh waves. Under these conditions the use of an S-I system could conceivably transform a so-called seismically noisy site into a moderately quiet one, at a relatively low cost.

Realization of this capability would greatly increase the flexibility of the deployment strategy underlying the installation of a regional underground nuclear test monitoring system. For this reason we conclude that development of an advanced S-I system is sufficiently important as to justify the fabrication of one or more engineering models for the purpose of additional evaluation of this particular P wave SNR enhancement technique.

8. REFERENCES

Abo-Zena, Anas, 1979, Dispersion function computations for unlimited frequency values, Geophys. J. R. Astr. Soc., 58, p. 91-105.

Asten, M. W., 1978, Geological control on three-component spectra of Rayleigh wave microseisms, Bull. Seis. Soc. Am., 68, p. 1623-1636.

Capon, J., 1969, High resolution frequency-wavenumber spectrum analysis, Proc. IEEE 57, p. 1408-1414.

_____, 1973, Analysis of microseismic noise at LASA, NORSAR and ALPA, Geophys. J. Royal Astr. Soc., 39, p. 39-54.

Clacy, G. R. T., 1968, Geothermal ground noise and frequency spectra in New Zealand volcanic region, J. Geophys. Res., 73, p. 5377-5383.

Douze, E. J., 1964, Noise attenuation in shallow holes, Teledyne Geotech, Technical Report 64-135, 29 p.

_____, 1967, Short-period seismic noise, Bull. Seis. Soc. Am., 57, p. 55-81.

_____, and G. G. Sorrells, 1972, Geothermal ground noise surveys, Geophysics, 37, p. 813-84.

Fix, J. E., 1972, Ambient earth motion in the period range from 0.1 to 2560 sec., Bull. Seis. Soc. Am., 62, p. 1753-1760.

Frantti, G. E., D. E. Willis, and J. T. Wilson, 1962, The spectrum of seismic noise, Bull. Seis. Soc. Am., 52, p. 113-121.

Goforth, T. T., E. J. Douze, and G. G. Sorrells, 1972, Seismic noise measurements in a geothermal area, Geophys. Prosp., 60, p. 926-935.

Haubrich, R. A., and K. McCamy, 1969, Microseisms: coastal and pelagic sources, Rev. of Geophys., 70, p. 539-571.

Isacks, B. and J. Oliver, 1964, Seismic waves with frequencies from 1 to 100 cycles per second recorded in a deep mine in northern New Jersey, J. Geophys. Res., 54, p. 1941-1979.

Iyer, H. M., and J. M. Healy, 1972, Evidence for the existence of locally-generated body waves in the short period noise at the large aperture seismic array, Montana, Bull. Seis. Soc. Am., 62, p. 13-29.

_____, and T. Hitchcock, 1974, Seismic noise measurements in Yellowstone Park, Geophysics, 39, p. 389-400.

_____, 1976, Seismic noise survey in Long Valley, California, J. Geophys. Res., 81, p. 821-840.

REFERENCES (Continued)

Lacoss, R. T., E. J. Kelley, and M. N. Toksoz, 1969, Estimation of seismic noise structure using arrays, Geophysics, 34, p. 21-38.

Liaw, Alfred L., 1977, Microseisms in geothermal exploration: studies in Grass Valley, Nevada, Lawrence Berkeley Laboratory Rept. 7002, 181 pp.

Liaw, A. L., and T. V. McEvilly, 1979, Microseisms in geothermal exploration-studies in Grass Valley, Nevada, Geophysics, 44, p. 1097-1115.

Mrazek, C. P., Z. A. Der, B. W. Barker and A. O'Donnell, 1979, Mode of propagation and coherence structure of the regional phases P_n, $\overline{P}$ and L_g and optimum array configurations for their enhancement, paper delivered at DARPA Program Review - Regional Seismic Detection and Discrimination.

Robertson, H., 1965, Physical and topographic factors as related to short period wind noise, Bull. Seis. Soc. Am., 55, p. 863-877.

Romney, Carl, 1964, Combinations of strain and pendulum seismographs for increasing the detectability of P: Bull. Seism. Soc. Am., v. 54, no. 6B, p. 2165-2174.

Sanford, A. R., A. G. Carapetian, and L. T. Long, 1968, High frequency microseisms from a known source. Bull. Seis. Soc. Am., 58, p. 325-338.

Shopland, Robert C., 1966, Shallow strain seismograph installation at the Wichita Mountains Seismological Observatory: Bull. Seism. Soc. Am., vol. 56, no. 2, p. 337-360.

Shopland, Robert C., 1968, Final Report, Project VT/5081, Multicomponent strain seismograph, 1 July 1965 to 31 December 1967, Technical Report No. 68-3: Garland, Geotech, A Teledyne Company, 156 p., 2 app.

Shopland, Robert C., and Richard H. Kirklin, 1969, Application of strain seismographs to the discrimination of seismic waves: Bull. Seism. Soc. Am., v. 59, p. 673-689.

Shopland, Robert C., and Richard H. Kirklin, 1970, Application of a vertical strain seismograph to the enhancement of P waves: Bull. Seism. Soc. Am., v. 60, p. 105-124.

Sorrells, G. G., 1971, A preliminary investigation into the relationship between long-period noise and local fluctuations in the atmospheric pressure field, Geophys. J. of the Royal Astr. Soc., 26, p. 71-82.

Toksoz, M. N., and R. T. Lacoss, 1968, Microseisms: Mode structure and sources, Science, 159, p. 872-873.

Whiteford, P. C., 1970, Ground movement in Waiotapu geothermal region, New Zealand, Geothermics (special issue on proceedings of the U. S. Sym. Div. Util. of Geothermal Resources), 2 (Part III), p. 478-486.

REFERENCES (Continued)

_____, 1975, Studies of the propagation and source locations of geothermal seismic noise, 2nd U. S. Symposium on the Dev. and Use of Geothermal Resources, San Francisco, p. 1263-1271.

APPENDIX TO TECHNICAL REPORT NO. 80-6

STRAIN-INERTIAL SNR ENHANCEMENT USING A PREDICTION ERROR FILTER

STRAIN-INERTIAL SNR ENHANCEMENT USING A PREDICTION ERROR FILTER

1. FILTER DESIGN

Let $n_i(t)$ and $n_e(t)$ be the outputs of colocated inertial and strain sensors when only background noise is present. We wish to apply a filter to the strain output in order to predict the background noise on the inertial transducer.

Let $\hat{n}_i(t)$ be the prediction of $n_i(t)$. Then

$$\hat{n}_i(t) = \int_{-\infty}^{\infty} h(\tau)\, n_e(t-\tau)\, d\tau \qquad 1.1$$

where $h(\tau)$ is the impulse response of the prediction filter. We will choose the filter properties such that

$$E\left\{\left(n_i(t) - \hat{n}_i(t)\right)^2\right\} = \text{minimum} \qquad 1.2$$

Applying this constraint in the frequency domain requires that the function

$$E(\omega) = \phi^n_{ii}(\omega) + |H(\omega)|^2 \phi^n_{ee}(\omega) - H^*(\omega)\, \phi^n_{ei}(\omega) - H(\omega)\, \phi^n_{ei}{}^*(\omega), \qquad 1.3$$

be minimized, where $\phi^n_{ii}(\omega)$ are the power densities of the noise at the output of the strain and inertial sensors, $\phi^n_{ei}(\omega)$ is the cross power spectral density relating the two outputs and $H(\omega)$ is the frequency response of the desired filter. Applying this constraint yields

$$\phi^n_{ei}(\omega) + \phi^n_{ei}(\omega) - H^*(\omega)\, \phi^n_{ii}(\omega) - H(\omega)\, \phi^n_{ee}(\omega) = 0$$

$$-\phi^n_{ei}(\omega) + j\phi^n_{ei}{}^*(\omega) - jH^*(\omega)\, \phi^n_{ii}(\omega) - jH(\omega)\, \phi^n_{ee}(\omega) = 0, \qquad 1.4$$

which have the solution

$$H(\omega) = \frac{\phi^n_{ei}(\omega)}{\phi^n_{ee}(\omega)} \qquad 1.5$$

Substitution of eq. 1.5 into eq. 1.3 yields

$$E(\omega) = \phi^{n}_{ii}(\omega) \left\{ 1 - \frac{| \phi^{n}_{ei}(\omega) |^2}{\phi^{n}_{ii}(\omega)\ \phi^{n}_{ee}(\omega)} \right\}$$

$$= \phi^{n}_{ii}(\omega) \left\{ 1 - \gamma^2_{ei}(\omega) \right\} \qquad 1.6$$

where $\gamma^2_{ei}(\omega)$ is the square of the simple coherence between the strain and inertial outputs. $E(\omega)$ in this case is seen to be the power spectral density of noise remaining after subtracting $\hat{n}_i(t)$ from $n_i(t)$. Clearly if the noise at the output of the strain and inertial transducers is perfectly coherent the inertial noise can be completely eliminated by this process.

2. SNR ENHANCEMENT

Let y_i (t) and y_e (t) be the outputs of the inertial and strain sensors when both noise and signal are present. Then

$$y_i\ (t) = s_i\ (t) + n_i\ (t)$$
$$y_e\ (t) = s_e\ (t) + n_i\ (t) \qquad 2.1$$

Let $\hat{y}_i$ (t) be the strain output after application of the noise prediction filter, i.e.

$$\hat{y}_i\ (t) = \int_{-\infty}^{\infty} h\ (\tau)\ y_e\ (t-\tau)\ d\tau \qquad 2.2$$

$$= \int_{-\infty}^{\infty} h\ (\tau)\ s_e\ (t-\tau)\ d\tau + \int_{-\infty}^{\infty} h\ (\tau)\ n_i\ (t-\tau)\ d\tau$$

Let ϵ (t) be the difference between the inertial output and the filtered strain output. Then

$$\epsilon\ (t) = s_i\ (t) - \int_{-\infty}^{\infty} h\ (\tau)\ s_e\ (t-\tau)\ d\tau$$

$$+ n_i\ (t) - \int_{-\infty}^{\infty} h\ (\tau)\ n_e\ (t-\tau)\ d\tau \qquad 2.3$$

Let ϕ^s_{ii} (ω) and ϕ^s_{ee} (ω) be the power spectra of the signal and the outputs of the inertial and strain sensors, respectively. Let ϕ^s_{ei} (ω) be the crosspower spectrum between the signal at the strain and inertial outputs. Then the power spectrum of the signal after completion of prediction error processing is

$$S\ (\omega) = \phi^s_{ii}\ (\omega) + |H\ (\omega)|^2\ \phi^s_{ee}\ (\omega) - H^*\ (\omega)\ \phi^s_{ei}\ (\omega) - H\ (\omega)\ \phi^{s*}_{ei}\ (\omega)$$

$$= \phi^s_{ii}\ (\omega)\ \left\{ 1 + |H\ (\omega)|^2\ \frac{\phi^s_{ee}(\omega)}{\phi^s_{ii}(\omega)} - H^*(\omega)\ \frac{\phi^s_{ei}(\omega)}{\phi^s_{ii}(\omega)} - H(\omega)\ \frac{\phi^{s*}_{ei}(\omega)}{\phi^s_{ii}(\omega)} \right\} \qquad 2.4$$

From eq. 1.6 the power spectrum of the noise after prediction error processing is

$$N(\omega) = E(\omega) = \phi^{n}_{ii}(\omega)\left(1-\gamma^{2}_{ei}(\omega)\right) \qquad 2.5$$

If $I(\omega)$ is the improvement in SNR after prediction error processing then

$$I(\omega) = \frac{S(\omega)}{N(\omega)} \Bigg/ \frac{\phi^{s}_{ii}(\omega)}{\phi^{n}_{ii}(\omega)}$$

$$= \frac{1}{1-\gamma^{2}_{ei}(\omega)} \left\{ 1 + \left| \frac{\phi^{n}_{ei}(\omega)}{\phi^{n}_{ee}(\omega)} \right|^{2} \left| \frac{\phi^{s}_{ee}(\omega)}{\phi^{s}_{ii}(\omega)} \right|^{2} - 2\mathrm{Re}\left(\frac{\phi^{n}_{ei}(\omega)}{\phi^{n}_{ee}(\omega)} \frac{\phi^{s*}_{ei}(\omega)}{\phi^{s}_{ii}(\omega)} \right) \right\} \qquad 2.6$$

3. CONCEPTUAL MODELS

3.1 P WAVE SIGNALS IN A HOMOGENEOUS, ISOTROPIC ELASTIC HALF SPACE

Let λ and μ be the constants specifying the elastic properties of the half space and assume a plane P wave is incident at the free surface. Let ζ and ψ be the velocity potentials satisfying the wave equations.

$$\nabla^2\zeta = \frac{1}{\alpha^2} \frac{\delta^2\zeta}{\delta t^2}$$

$$\nabla^2\psi = \frac{1}{\beta^2} \frac{\delta^2\psi}{\delta t^2} \qquad 3.1$$

where α and β are the P and S velocities in the medium. For an incident P wave these potentials have the form

$$\zeta = \left\{A_1 \exp\left[jk\left(\gamma_\alpha z - x\right)\right] + A_2 \exp\left[jk\left(-\gamma_\alpha z - x\right)\right\} \exp\left(j\omega t\right)\right. \qquad 3.2$$

$$\psi = B_2 \exp\left[jk\left(-\gamma_\beta z - x\right)\right] \exp\left(j\omega t\right)$$

where k is the apparent horizontal wave number, z and x are Cartesian coordinates normal and parallel to the free surface and

$$\gamma_\alpha = \left(\left(\frac{c}{\alpha}\right)^2 - 1\right)^{1/2} \qquad 3.3$$

$$\gamma_\beta = \left(\left(\frac{c}{\beta}\right)^2 - 1\right)^{1/2} \qquad 3.4$$

c is the apparent horizontal velocity which is defined by

$$c = \frac{\alpha}{\sin\theta} \qquad 3.5$$

where θ is the angle of incidence.

We are principally interested in the vertical displacements and vertical strains. The vertical displacement, W, and the vertical strain $\frac{\delta W}{\delta z}$ are related to the potentials ζ, ψ through

$$W = \frac{\delta \zeta}{\delta z} + \frac{\delta \psi}{\delta x} \tag{3.6}$$

$$\frac{\delta W}{\delta z} = \frac{\delta^2 \zeta}{\delta z^2} + \frac{\delta^2 \psi}{\delta x^2} \tag{3.7}$$

while the normal and tangential stresses acting in planes parallel to the free surface are related to the potentials through

$$\sigma_{zx} = \mu \left(\frac{\delta^2 \zeta}{\delta x \delta z} + \frac{\delta^2 \psi}{\delta x^2} - \frac{\delta^2 \psi}{\delta z^2} \right) \tag{3.8}$$

$$\sigma_{zz} = \lambda \nabla^2 \zeta + 2\mu \left(\frac{\delta^2 \zeta}{\delta z^2} + \frac{\delta^2 \psi}{\delta x \delta z} \right) \tag{3.9}$$

Imposing the condition that the stresses must vanish at the free surface results in the following expressions for the reflection coefficients A_2 and B_2.

$$A_2 = A_1 \left\{ \frac{4\left(\frac{c^2}{\alpha^2} - 1\right)^{1/2} \left(\frac{c^2}{\beta^2} - 1\right)^{1/2} - \left(\frac{c^2}{\beta^2} - 2\right)^2}{4\left(\frac{c^2}{\alpha^2} - 1\right)^{1/2} \left(\frac{c^2}{\beta^2} - 1\right)^{1/2} + \left(\frac{c^2}{\beta^2} - 2\right)^2} \right\} \tag{3.10}$$

$$= A_1 \Gamma \tag{3.11}$$

$$B_2 = A_1 \left\{ \frac{-4\left(\frac{c^2}{\alpha^2} - 1\right)^{1/2} \left(\frac{c^2}{\beta^2} - 2\right)}{4\left(\frac{c^2}{\alpha^2} - 1\right)^{1/2} \left(\frac{c^2}{\beta^2} - 1\right)^{1/2} + \left(\frac{c^2}{\beta^2} - 2\right)^2} \right\} \tag{3.12}$$

$$= -A_1 \Omega \tag{3.13}$$

Using equations 3.1, 3.2, and 3.10-3.13 in equations 3.6 and 3.7 the expressions for the vertical displacements and vertical strains are found to be

$$W = jkA_1 \left\{ \gamma_\alpha \left[\exp(jk\gamma_\alpha z) - \Gamma \exp(-jk\gamma_\alpha z) \right] - \Omega \exp(-jk\gamma_\beta z) \right\} \exp\left(j(\omega t - kx)\right) \qquad 3.14$$

$$\frac{\delta W}{\delta z} = k^2 A_1 \left\{ \gamma_\alpha^2 \left[\exp(jk\gamma_\alpha z) + \Gamma \exp(-jk\gamma_\alpha z) \right] + \gamma_\beta \Omega \exp(-jk\gamma_\beta z) \right\} \exp\left(j(\omega t - kx)\right) \qquad 3.15$$

3.2 RAYLEIGH WAVES IN A HOMOGENEOUS, ISOTROPIC, ELASTIC HALF SPACE

For the purposes of this investigation it is sufficient to restrict our attention to the vertical displacements and strains created by surface point loads. Following the development in Ewing et al (1954) let us choose a cylindrical coordinate system (r, θ, z) and displacement potentials of the form

$$\begin{aligned} \zeta &= Ae^{-\nu z} H_0^{(2)}(kr) \\ \psi &= Be^{-\nu' z} H_0^{(2)}(kr) \end{aligned} \qquad 3.16$$

where

$$\begin{aligned} \nu^2 &= k^2 - k_\alpha^2 \\ (\nu')^2 &= k^2 - k_\beta^2 \end{aligned} \qquad 3.17$$

$$\begin{aligned} k_\beta^2 &= \frac{\omega^2}{\alpha^2} \\ k_\beta^2 &= \frac{\omega^2}{\beta^2} \end{aligned} \qquad 3.18$$

and $H_0^{(2)}(kr)$ is a Hankel function of the second kind and zero order.

Let q and W be the radial and vertical displacements respectively. Then in terms of the potentials

$$\begin{aligned} q &= \frac{\delta \zeta}{\delta r} + \frac{\delta^2 \psi}{\delta r \delta z} \\ W &= \frac{\delta \zeta}{\delta z} - \frac{1}{r} \frac{\delta}{\delta r}\left(r \frac{\delta \psi}{\delta r} \right) \end{aligned} \qquad 3.19$$

Now the normal and tangential stresses acting on planes parallel to the free surface are related to the displacements through

$$\sigma_{zr} = \mu \left(\frac{\delta q}{\delta z} + \frac{\delta w}{\delta r} \right)$$

$$\sigma_{zz} = \lambda\theta + 2\mu \frac{\delta w}{\delta z} \qquad 3.20$$

where

$$\theta = \frac{1}{r} \frac{\delta}{\delta r} \left(\frac{r\delta\zeta}{\delta r} \right) + \frac{\delta^2 \zeta}{\delta z^2} \qquad 3.21$$

Using equations 3.16 through 3.19 in equation 3.20 yields

$$\sigma_{zr} = \mu \left[2k\nu A - k (2k^2 - k^2_\beta) B \right] H^2_1 (kr)$$

$$\sigma_{zz} = \mu \left[(2k^2 - k^2_\beta) A - 2k^2 \nu' B \right] H^2_0 (kr), \qquad 3.22$$

at $z = 0$

Now suppose a vertical point force of strength $ZH^2_0 (kr)$ is applied at the origin. Then

$$\sigma_{zr}]_{z=0} = 0$$

$$\sigma_{zz}]_{z=0} = Z H^2_0 (kr) \qquad 3.23$$

and equations 3.22 become

$$-2 \nu A + 2 (k^2 - k^2_\beta) B = 0$$

$$(2k^2 - k^2_\beta) A - 2k^2 \nu' B = \frac{Z}{\mu} \qquad 3.24$$

Solving equations 3.24 leads to the following expressions for A and B

$$A = \frac{(2k^2-k_\beta^2)}{F(k)} \frac{Z}{\mu}$$

$$B = \frac{2\nu}{F(k)} \frac{Z}{\mu} , \qquad 3.25$$

where

$$F(k) = (2k^2-k_\beta^2)^2 - 4k^2\nu\nu' \qquad 3.26$$

Therefore

$$W = \frac{\nu\ (2k^2-k_\beta^2)e^{-\nu z} + 2k^2\nu^1\ e^{-\nu' z}}{F(k)} \frac{Z}{\mu} H_0^2(kr) \qquad 3.27$$

and

$$\frac{dW}{dZ} = \frac{\nu^2\ (2k^2-k_\beta^2) - 2k^2\nu^1\nu\ e^{-\nu' z}}{F(k)} \frac{Z}{\mu} H_0^2\ (kr)$$

In order to obtain the point force solutions Z is replaced by $-\frac{1\ kdk}{2\pi}$ in equations 3.27 and the resulting expressions are integrated with respect to k in the interval $0 \leq k \leq \infty$, i.e.

$$W = \frac{1}{2\pi\mu}\int_0^\infty \frac{\nu\ [(2k^2-k_\beta^2)\ e^{-\nu z} + 2k^2\ e^{-\nu' z}]}{F(k)} H_0^2\ (kr)\ kdk \qquad 3.28$$

$$\frac{dW}{dZ} = \frac{-1}{2\pi}\int_0^\infty \frac{\nu\ [\nu\ (2k^2-k_\beta^2)\ e^{-\nu z} - 2k^2\nu^1\ e^{-\nu' z}]}{F(k)} H_0^2\ (kr)\ kdk$$

Let W_R and $\frac{dW_R}{\delta z}$ be the Rayleigh wave vertical displacements and strains and let K_R be a real solution to the equation

$$F(k) = 0 \tag{3.29}$$

then

$$W_R = \frac{jL}{\mu} \left\{ \frac{K_R \nu \left[(2K_R^2 - k_\beta^2)\, e^{-\nu z} + 2K_R^2\, e^{-\nu' z} \right]}{F'(K_R)} \right\} H_0^2 (K_R r) \tag{3.30}$$

$$\frac{\delta W_R}{\delta z} = \frac{-jL}{\mu} \left\{ \frac{K_R \nu \left[\nu (2K_R^2 - k_\beta^2)\, e^{-\nu z} - 2K_R^2 \nu'\, e^{-\nu' z} \right]}{F'(K_R)} \right\} H_0^2 (K_R r)$$

where now

$$\nu = (K_R^2 - k^2\alpha)^{1/2}$$
$$\nu' = (K_R^2 - k_\beta^2)^{1/2} \tag{3.31}$$

and $F'(K_R) = \frac{\delta}{\delta k} F(k) \Big]_{k = K_R}$

$$= 4K_R \left\{ 4K_R^2 - 2k_\beta^2 - \left(2\nu\nu' + K_R^2 \frac{\nu'}{\nu} + k_R^2 \frac{\nu}{\nu'} \right) \right\} \tag{3.32}$$

For the purposes of this investigation we are principally interested in the contributions from remote sources. Thus for $K_R r >> 1$

$$H_0^2 (K_R r) \approx \left(\frac{2}{\pi K_R r} \right)^{1/2} \exp \left(\frac{i\pi}{4} \right) \exp (-j K_R r) \tag{3.33}$$

and

$$W_R \approx \frac{j}{\mu} \left(\frac{2}{\pi} \right)^{1/2} \frac{L}{r^{1/2}} \left\{ \frac{K_R^{1/2}\, \nu \left[(2K_R^2 - k_\beta^2)\, e^{-\nu z} + 2K_R^2\, e^{-\nu' z} \right]}{F'(K_R)} \right\} \exp \left[-j \left(K_R r - \frac{\pi}{4} \right) \right]$$

$$\frac{\delta W_R}{\delta z} \approx \frac{-j}{\mu} \left(\frac{2}{\pi} \right)^{1/2} \left(\frac{L}{r^{1/2}} \right) \left\{ \frac{K_R^{1/2} \nu \left[\nu (2K_R^2 - k_\beta^2)\, e^{-\nu z} - 2K_R^2 \nu'\, e^{-\nu' z} \right]}{F'(K_R)} \right\} \exp \left[-j \left(K_R r - \frac{\pi}{4} \right) \right] \tag{3.34}$$

4. POWER AND CROSS POWER SPECTRA FOR IDEALIZED NOISE FIELDS

4.1 SCATTERED P WAVE NOISE FIELD

Let us consider a noise field that consists solely of scattered P waves with apparent horizontal phase velocities ranging from ∞ to c_{min} where

$$c_{min} \leq \alpha \tag{4.1}$$

Let us further require that the incident P wave field be laterally homogeneous, isotropic, and that its potential amplitude be independent of the apparent horizontal phase velocity. If $N_{DD}(\vec{k},\omega,z)$ is the 3 dimensional displacement power spectrum of this field then

$$\begin{aligned} N_{DD}(\vec{k},\omega,z) &= |A_1(\theta,\omega)|^2 \; |D(k,z)|^2 \quad |\vec{k}| \leq \frac{\omega}{c_{min}} \\ &= 0 \qquad\qquad\qquad\qquad |\vec{k}| < \frac{\omega}{c_{min}} \end{aligned} \tag{4.2}$$

where from eq. 3.14

$$D(k,z) = jk \left\{ \gamma_\alpha \left[\exp(jk\gamma_\alpha z) - \Gamma \exp(-jk\gamma_\alpha z)\right] - \Omega \exp(-jk\gamma_\beta z) \right\} \tag{4.3}$$

and from equations 3.10 through 3.13

$$\Gamma = \frac{4k^2 (k_\alpha^2 - k^2)^{1/2} (k_\beta^2 - k^2)^{1/2} - (k_\beta^2 - 2k^2)^2}{4k^2 (k_\alpha^2 - k^2)^{1/2} (k_\beta^2 - k^2)^{1/2} + (k_\beta^2 - 2k^2)^2} \tag{4.4}$$

$$\Omega = \frac{4k (k_\alpha^2 - k^2)^{1/2} (k_\beta^2 - 2k^2)}{4k^2 (k_\alpha^2 - k^2)^{1/2} (k_\beta^2 - k^2)^{1/2} - (k_\beta^2 - 2k^2)^2} \tag{4.5}$$

Similarly if $N_{EE}\ (k,\omega,z)$ is the 3 dimensional vertical strain power spectrum then

$$N_{EE}\ (\vec{k},\omega,z) = |A_1(\theta,\omega)|^2\ |S\ (\vec{k},z)|^2 \qquad |\vec{k}| \leq \frac{\omega}{c_{min}}$$
$$= 0 \qquad |\vec{k}| > \frac{\omega}{c_{min}} \qquad 4.6$$

where from equation 3.15

$$\frac{\delta D}{\delta z}\ (\vec{k},z) = -\left\{(k_\alpha^2 - k^2)\left(\exp\ [j\ (k_\alpha^2 - k^2)^{1/2}\ Z] + \Gamma\ \exp\ [-j\ (k_\alpha^2 - k^2)^{1/2} z]\right)\right.$$
$$\left. + k\ (k_\beta^2 - k^2)^{1/2}\left(\exp\ [-j\ (k_\beta^2 - k^2)\ z]\right)\right\} \qquad 4.7$$

Finally if $N_{ED}\ (\vec{k},\omega,z)$ is the 3 dimensional vertical strain-vertical displacement cross power spectrum then

$$N_{ED}\ (\vec{k},\omega,z) = \frac{\delta D}{\delta z}(\vec{k},z)\ D^*(\vec{k},z) \qquad |\vec{k}| \leq \frac{\omega}{c_{min}}$$
$$= 0 \qquad |\vec{k}| > \frac{\omega}{c_{min}} \qquad 4.8$$

4.2 RAYLEIGH WAVE, NOISE FROM SCATTERED, REMOTE SURFACE SOURCES

Let $\vec{r}$ be the radius vector from an arbitrarily chosen origin to an observation point. Let $\vec{r}'$ be the radius vector from the origin to a point surface source of Rayleigh waves. From equation 3.34 the Fourier time transform of the vertical displacement component of the Rayleigh wave

$$W_R\ (\vec{r},\vec{r}'\ \omega;K_R) = \frac{L\ (\omega,\vec{r}')}{|\vec{r}-\vec{r}'|^{1/2}}\ G\ (K_R,z)\ \exp\ (j\tfrac{\pi}{4})\ \exp\left(-jK_R\ |\vec{r}-\vec{r}'|\right) \qquad 4.9$$

Let us now impose the restriction that $|\vec{r}'| >> |r|$. Then

$$K_R\,|\vec{r}-r'| \approx K_R r' - K_R r\cos(\theta-\theta') \qquad 4.10$$

and

$$\frac{1}{|r-r'|^{1/2}} \approx \frac{1}{(r')^{1/2}} \qquad 4.11$$

where r,θ are the polar coordinates of the observation point and r',θ' are the polar coordinates of the source.

Therefore

$$W(\vec{r},\vec{r}',\omega;K_R) \approx \frac{L(\omega,r';\theta')}{(r')^{1/2}}\,G(K_R,Z)\exp\left(j\frac{\pi}{4} - K_R r' - K_R r\cos(\theta-\theta')\right) \qquad 4.12$$

Now let us consider a continuous isotropic source distribution in the interval $a < r' < b$, W_r then may be expressed as

$$W_R = G(K_R,Z)e^{j\frac{\pi}{4}}\int_0^{2\pi}\exp\left(-jK_R r\cos(\theta-\theta')\right)d\theta'\int_a^b (r')^{1/2}L(\omega,r')\exp(-jK_R r')dr'$$

$$= G(K_R,Z)e^{j\frac{\pi}{4}}J_0(K_R r)\,\bar{L}(\omega,K_R;a,b) \qquad 4.13$$

where

$$\bar{L}(\omega,K_R;a,b) = \int_a^b (r')^{1/2}L(\omega,r')\exp(-jK_R r')\,dr' \qquad 4.14$$

Now let us assume that the vertical strain field is observed at the point defined by the radius vector $\vec{r} + \delta\vec{r}$. Then by analogy with the previous arguments

$$\frac{\delta W_R}{\delta Z} = \frac{\delta G(K_R,Z)}{\delta Z}\,e^{j\frac{\pi}{4}}\,J_0(K_R|\vec{r}+\delta\vec{r}|)\,\bar{L}(\omega,K_R;a,b) \qquad 4.15$$

If ϕ_{ei} is the cross power spectral density relating the strain observations at $\vec{r} + \delta\vec{r}$ to the displacement observations at r then

$$\phi_{ei} = \frac{\delta W_R}{\delta z} \quad W_R^* \tag{4.16}$$

$$= |\bar{L}|^2 = G * \frac{\delta G}{\delta z} \; J_0 \; (K_R r) \; J_0 \; (K_R \; |\vec{r} + \delta\vec{r}|) \tag{4.17}$$

Now moving the vertical displacement point to the origin yields

$$\phi_{ei} = |\bar{L}|^2 \; G^* \; \frac{\delta G}{\delta z} \; J_0(K_R \; \delta r) \tag{4.18}$$

By similar arguments the power spectral density of the displacements, ϕ_{ii}, and the power spectral density of the strains are found to be

$$\phi_{ii} = |\bar{L}|^2 \; |G|^2 \tag{4.19}$$

$$\phi_{ee} = |\bar{L}|^2 \; |\frac{\delta G}{\delta z}|^2 \tag{4.20}$$

5. NOISE REDUCTION IN MULTICOMPONENT FIELDS

5.1 SCATTERED RAYLEIGH WAVES CONTAMINATED BY STRAIN SYSTEM NOISE

Let R be the ratio of the noise power at the output of the prediction error processor relative to the noise at the output of the inertial sensor. Then according to this definition complete noise rejection is achieved when R = 0 and increasingly greater amounts of noise are passed by the processor as $R \to 1$. From equation 1.6

$$R = 1 - \gamma_{ei}^2 \tag{5.1}$$

Let us assume now that the earth noise consists entirely of Rayleigh waves from scattered surface sources and that the data observed at the output of the strain sensor are contaminated by system noise. If the strain and intertial sensors are colocated, then from equations 4.17 through 4.19 relevant power and cross power spectral densities are given by

$$\phi_{ii} = |\bar{L}|^2 \, |G|^2 \tag{5.2}$$

$$\phi_{ee} = |\bar{L}|^2 \, |G|^2 + |N_s|^2 \tag{5.3}$$

$$\phi_{ei} = |\bar{L}|^2 \, G^* \frac{\delta G}{\delta Z} \tag{5.4}$$

where $|N_s|^2$ is the system noise power at the output of the strain sensor. Therefore in this case γ_{ei}^2 is given by

$$\gamma_{ei}^2 = \frac{|\bar{L}|^4 \, |G|^2 \left|\frac{\delta G}{\delta Z}\right|^2}{|\bar{L}^4| \, |G|^2 \left|\frac{\delta G}{\delta Z}\right|^2} \left(1 + \frac{|N_s|^2}{|\bar{L}|^2 \left|\frac{\delta G}{\delta Z}\right|^2}\right) \tag{5.5, 5.6}$$

$$= \frac{1}{1+A}$$

Let B define the ratio of system noise to total noise power at the output of the strain sensor. Then

$$B = \frac{|N_S|^2}{|\bar{L}|^2 \left|\frac{\delta G}{\delta Z}\right|^2 + |N_S|^2} \qquad 5.7$$

and

$$A = \frac{B}{1-B} \qquad 5.8$$

Therefore

$$\gamma_{ei}^2 = 1-B \qquad 5.9$$

and

$$R = B \qquad 5.10$$

In other words in this particular case the reduction in noise achieved through prediction error filtering using a linear combination of the outputs of strain and inertial sensors is limited only by the presence of system noise at the strain output.

5.2 SCATTERED RAYLEIGH WAVES CONTAMINATED BY WIND NOISE

In this case let the power spectra of the Rayleigh wave noise at the output of the inertial and strain sensors be denoted by $|W_R|^2$ and $|W_R'|^2$ respectively. Similarly let $|W_w|^2$ and $|W_w'|^2$ be the power spectra of the wind noise at the outputs of the inertial and strain sensors. Furthermore let us define the ratios Q and T by

$$Q^2 = \frac{|W_w|^2}{|W_w'|^2} \qquad 5.11$$

$$T^2 = \frac{|W_R|^2}{|W_R'|^2}$$

From arguments presented by Sorrells (1971) Q^2 can be shown to be given by

$$Q^2 = \frac{|H|^2}{\left|\frac{\delta H}{\delta Z}\right|^2} \qquad 5.12$$

where H is the quasi static vertical displacement response of the earth to atmospheric pressure variations and $\frac{\delta H}{\delta Z}$ is the vertical strain response. For observations at the surface of a perfectly elastic, homogeneous and isotropic half space

$$H = \frac{-1}{2\mu} \frac{c_0}{\omega} \left(\frac{\lambda+2\mu}{\lambda+\mu}\right) \qquad 5.13$$

$$\frac{\delta H}{\delta Z} = \frac{1}{2\mu} \left(\frac{\mu}{\lambda+\mu}\right)$$

where C is the local wind speed. Therefore

$$Q^2 = \frac{c^2}{\omega^2} \left(\frac{\alpha^2}{\beta^2}\right)^2 \qquad 5.14$$

From equations 3.34

$$T^2 = \left\{ \frac{-(2K_R^2 - k_\beta^2) + 2K_R^2}{\nu(2K_R^2 - k_\beta^2) - 2K_R^2 \nu'} \right\}^2 \qquad 5.15$$

and for the case where $\lambda = \mu$

$$T^2 \approx \frac{16\beta^2}{\omega^2} \qquad 5.16$$

Now using equations 5.11 to express the inertial spectral components in terms of their strain counterparts it is easy to show that in this case γ_{ei}^2 is given by

$$\gamma_{ei}^2 = \frac{\left(Q|W_w'|^2 + T|W_R'|^2\right)}{\left(Q|W_w'|^2 + T|W_R'|^2\right)^2 + (Q-T)|W_w'|^2|W_R'|^2} \qquad 5.17$$

Then letting B be the ratio of wind noise power to total noise power at the output of the strain sensor; i.e

$$B = \frac{|W_w'|^2}{|W_w'|^2 + |W_R'|^2} \quad , \qquad 5.18$$

it can be shown that

$$R = 1 - \gamma_{ei}^2 = \frac{\left(1-\frac{Q}{T}\right)^2 B(1-B)}{\left(1-\frac{Q}{T}\right)^2 B(1-B) + \left[1- \left(1-\frac{Q}{T}\right) B\right]^2} \qquad 5.19$$

and from equations 5.14 and 5.16

$$\frac{Q}{T} \simeq \frac{c}{16\beta} \qquad 5.20$$

Now c is generally of the order of meters/sec while β is of the order of kilometers/sec. Thus

$$\frac{Q}{T} = 0\ (10^{-3}) \qquad 5.21$$

Therefore

$$1 - \frac{Q}{T} \simeq 1 \qquad 5.22$$

and for $B < 1$

$$R \simeq B \qquad 5.23$$

In other words for small values of B, the addition of wind noise to the Rayleigh wave field is comparable to the addition strain system noise, insofar as its impact on the noise reducing capabilities of a two channel strain inertial processing system is concerned. Notice that this approximation is no longer valid for values of B near 1, i.e., when the strain noise is completely saturated by the wind induced component. Under these conditions it is convenient to write R as

$$R = \frac{\zeta^2 \ (1 - \delta B) \ \delta B}{\zeta^2 \ (1-\delta B) \ \delta B + [1-\zeta \ (1-\delta B)]^2} \qquad 5.24$$

where

$$\zeta = 1 - \frac{Q}{T}$$

and

$$B = 1 - \delta B$$

Assuming $\delta B << 1$ then equation 5.24 can be approximated by

$$R \simeq \frac{1}{1 + \left(\frac{1-\zeta}{\zeta}\right)^2 \frac{1}{\delta B}} \qquad 5.25$$

$$\simeq \frac{\delta B}{\delta B + \left(\frac{\frac{Q}{T}}{1 - \frac{Q}{T}}\right)^2}$$

which shows that $R \to 0$ as $\delta B \to 0$ for $\frac{Q}{T} \neq 0$

Summarizing then

$$R \simeq B \qquad B \ll 1 \qquad 5.26$$

$$R \to 0 \text{ as } B \to 0$$

and

$$R \simeq \frac{1 - B}{1-B + \left(\frac{\frac{Q}{T}}{1 - \frac{Q}{T}}\right)^2} \qquad 5.27$$

$$R \to 0 \text{ as } B \to 1$$

Equations 5.26 and 5.27 state that the noise rejection provided by a strain inertial system will be complete only if the noise at the output of the strain transducer consists of either pure Rayleigh wave noise or pure wind generated noise. Otherwise the noise reducing capabilities of the system will be functinally dependent on the percentage of wind noise in the noise observed at the output of the strain sensor.

Finally it can be readily shown that R has a maximum value at

$$B = \frac{1}{2-\zeta} = \frac{1}{1+\frac{Q}{T}} \qquad 5.28$$

at this point

$$R_{max} = \left(\frac{\zeta}{2-\zeta}\right)^2 = \left(\frac{1-\frac{Q}{T}}{1+\frac{Q}{T}}\right)^2 \qquad 5.29$$

For the case of Rayleigh waves contaminated by wind noise the maximum value of R occurs at B $\simeq$ 1 and at this point R max $\simeq$ 1. Thus except for a very small range of values near B = 1

$$R = B \qquad 0 \lesssim B \leq 1 \qquad 5.30$$

which is identical to the relationship found for the strain system noise.

5.3 SCATTERED RAYLEIGH WAVES CONTAMINATED BY P WAVES

An expression similar to 5.19 may be derived for the case where the propagating earth noise consists of both scattered P and Rayleigh waves. In this instance, however, it is instructive to express the noise reduction in terms of the ratio of the P wave noise power to the total noise power observed at the output of the inertial sensor.

Let B_p denote this ratio. Then

$$B_p = \frac{|W_p|^2}{|W_p|^2 + |W_R|^2} \qquad 5.31$$

where $|W_p|^2$ is the P wave spectral noise power.

Let the parameters P and V be defined by

$$|P|^2 = P^2 = \frac{|W_P'|^2}{|W_P|^2} \qquad 5.32$$

$$|V|^2 = V^2 = \frac{|W_R'|^2}{|W_R|^2} \qquad 5.33$$

where, as before, the primed quantities denote spectral densities at the output of the strain sensor.

Then it can be easily shown that

$$R = \frac{\left[1 + \left(\frac{P}{V}\right)^2\right] B_P \ (1-B_P)}{1 - \left[1 - \left(\frac{P}{V}\right)^2\right] B_P} \qquad 5.34$$

Now suppose we confine our attention to the case where the observations are made at the surface and the scattered P waves arrive at the site with near vertical angles of incidence. This approximates the so called "mantle P wave" noise field. Then

$$|P|^2 \simeq k^2 \left\{ \frac{\gamma_\alpha^2 \ (1 + \Gamma) + \gamma_\beta \ \Omega}{\gamma_\alpha (1 - \Gamma) - \Omega} \right\}^2 \qquad 5.35$$

where Γ and Ω are defined by equations 3.10 through 3.13

and assuming $\lambda = \mu$,

$$|P|^2 \simeq \frac{4}{9} \frac{\omega^2 \ \sin^2\theta}{\alpha^2} \left\{ \frac{3 \ \sin^2\theta - 1}{(3 \ \sin^2\theta - ^2)^2} \right\} \qquad 5.36$$

where θ is the angle of incidence for the P wave noise. Then using equation 5.16

$$|V|^2 = \frac{1}{T^2} \simeq \frac{\omega^2}{16\beta^2} \qquad 5.37$$

and

$$\frac{|P|^2}{|V|^2} = \frac{P^2}{V^2} \simeq \frac{16 \sin^2\theta \ (3 \sin^2 \theta - 1}{27 \left(\frac{3}{2} \sin^2 \theta - 1\right)^2} \qquad 5.38$$

If we confine our attention to near vertical angles of incidence $\eta << |$ and equation 5.37 reduces to

$$\frac{P^2}{V^2} \simeq \frac{16}{27} \theta^2 \qquad 5.39$$

and given this condition R reduces to

$$R \simeq B_P \ , \quad B_P \neq 1 \qquad 5.40$$

Near $B_P = 1$ we may replace B_P by $1-\delta B_P$ and neglecting power of $\delta B_P \geq 2$ one obtains

$$R \simeq \frac{\left(1 + \left(\frac{P}{V}\right)\right)^2 \delta B_P}{1 + \left[\left(\frac{P}{V}\right)^2 - 1\right] \delta B_P}$$

$$R \simeq \left(1 + \left(\frac{P}{V}\right)^2\right) \delta B_P \qquad 5.41$$

It should be noted that according to the definitions of B_P and δB_P

$$\delta B_P = \frac{|W_R|^2}{|W_P|^2 + |W_R|^2}$$

which is the fractional Rayleigh wave power at the output of the inertial sensor. Let this ratio be defined by B_R. Then equation 5.41 may be rewritten

$$R \simeq \left(1 + \left(\frac{P}{V}\right)^2\right) B_R \quad B_R \to 0 \qquad 5.42$$

It can be easily shown for this case that R has a maximum at

$$B_P = \frac{1}{1 + \frac{P}{V}} \qquad 5.43$$

and at this point

$$R = \frac{\left[1 + \left(\frac{P}{V}\right)^2\right]}{1 + \frac{P}{V}} \qquad 5.44$$

Since $\frac{P}{V} << 1$, R reduces to

$$R \approx 1 - \frac{|P|}{|V|} \qquad 5.45$$

Thus where the propagating major contains both Rayleigh wave and mantle P wave components, the strain inertial processing system will completely suppress the Rayleigh wave component in the interval $0 < Bp < 1 - \frac{|P|}{|V|}$. As B_p increases through $1 - \frac{|P|}{|V|}$ the system will begin to suppress the P wave component and total noise rejection is achieved at $B_p = 1$.

UNCLASSIFIED

SECURITY CLASSIFICATION OF THIS PAGE (When Data Entered)

REPORT DOCUMENTATION PAGE

READ INSTRUCTIONS BEFORE COMPLETING FORM

1. REPORT NUMBER: AFOSR-TR- 80-0633	2. GOVT ACCESSION NO.: AD-A088 357
3. RECIPIENT'S CATALOG NUMBER	
4. TITLE (and Subtitle): AN ASSESSMENT OF THE USE OF STRAIN AND INERTIAL SEISMOGRAPHS TO ENHANCE SEISMIC SIGNAL TO NOISE RATIOS	5. TYPE OF REPORT & PERIOD COVERED: Final
	6. PERFORMING ORG. REPORT NUMBER
7. AUTHOR(s): G G Sorrells, O D Starkey	8. CONTRACT OR GRANT NUMBER(s): F 49620-79-C-0015
9. PERFORMING ORGANIZATION NAME AND ADDRESS: Teledyne Geotech, 3401 Shiloh Road, Garland, Texas 75041	10. PROGRAM ELEMENT, PROJECT, TASK AREA & WORK UNIT NUMBERS: 62701E, AO 3291-30, 0F10
11. CONTROLLING OFFICE NAME AND ADDRESS: DARPA, 1400 Wilson Blvd, Arlington, VA 22209	12. REPORT DATE: Mar 80
	13. NUMBER OF PAGES: 53
14. MONITORING AGENCY NAME & ADDRESS (if different from Controlling Office): AFOSR/NP, Bolling AFB, Wash DC 20332	15. SECURITY CLASS. (of this report): unclassified
	15a. DECLASSIFICATION/DOWNGRADING SCHEDULE

16. DISTRIBUTION STATEMENT (of this Report)

Approved for public release;
Distribution unlimited.

17. DISTRIBUTION STATEMENT (of the abstract entered in Block 20, if different from Report)

18. SUPPLEMENTARY NOTES

19. KEY WORDS (Continue on reverse side if necessary and identify by block number)

20. ABSTRACT (Continue on reverse side if necessary and identify by block number)

Simple statistical models of the ambient earth noise field in a homogeneous isotropic, perfectly elastic solid were developed. The models include randomly scattered P waves, randomly scattered Sv waves and Rayleigh waves from random sources. The models are being used to evaluate use of a linear combination of the outputs of strain and inertial seismographs as a prediction error operator to enhance P wave signal to noise ratios. Linear combinations

DD FORM 1 JAN 73 1473 EDITION OF 1 NOV 65 IS OBSOLETE

UNCLASSIFIED

of the outputs of vertical strain and inertial seismographs are collocated at the surface of the earth. Preliminary results are broadly consistant with results obtained during earlier Teledyne Geotech experimental studies. In particular, it was found that in the case of pure fundamental mode Rayleigh wave noise, the performance of a strain inertial processor is independent of the source distribution and is limited only by the presence of system noise. Conversely, if ambient noise consists of pure P or S(v) waves, the performance of the strain inertial processor is dependent upon the correlation structure of the field, and under certain conditions, use of the strain inertial processor can result in a substantial degradation of P wave signal to noise ratios.